Computers and Chemical Engineering 126 (2019) 434–450

Contents lists available at ScienceDirect

Computers and Chemical Engineering

journal homepage: www.elsevier.com/locate/compchemeng

Output feedback stochastic nonlinear model predictive control for batch processes

Eric Bradford*, Lars Imsland

Engineering Cybernetics, Norwegian University of Science and Technology, Trondheim, Norway

ARTICLE INFO

Article history:
Received 17 February 2019
Revised 14 April 2019
Accepted 15 April 2019
Available online 25 April 2019

Keywords:
Model-based nonlinear control
Stochastic parameters
Uncertain dynamic systems
Polynomial chaos expansions
Polymerization
Probabilistic constraints

ABSTRACT

Batch processes play a vital role in the chemical industry, but are difficult to control due to highly nonlinear behaviour and unsteady state operation. Nonlinear model predictive control (NMPC) is therefore one of the few promising approaches. Batch process models are however often affected by uncertainties, which can lower the performance and cause constraint violations. In this paper we propose a shrinking horizon NMPC algorithm accounting for these uncertainties to optimize a probabilistic objective subject to chance constraints. At each sampling time only noisy output measurements are observed. Polynomial chaos expansions (PCE) are used to express the probability distributions of the uncertainties, which are updated at each sampling time using a PCE state estimator and exploited in the NMPC formulation. The approach considers feedback by using time-invariant linear feedback gains, which alleviates the conservativeness of the approach. The NMPC scheme is verified on a polymerization semi-batch reactor case study.

© 2019 Elsevier Ltd. All rights reserved.

1. Introduction

Batch processes are used in many sectors in the chemical industry due to their inherent flexibility to produce multiple products and deal with variations in feedstock, product specifications, and market demand. Batch processes are difficult to control due to frequently highly nonlinear behaviour and unsteady state operation leading to an increased acceptance of advanced control methods in industry (Nagy and Braatz, 2003). Model predictive control (MPC) is a popular advanced control method for multivariate plants with process constraints. At each sampling time MPC solves an optimal control problem (OCP) based on a dynamic plant model to evaluate a finite sequence of control actions (Maciejowski, 2002). Feedback is introduced to this procedure through the state update. Nonlinear MPC (NMPC) employs a nonlinear dynamic model to deal with systems that display strong nonlinear behaviour. In particular, the use of first principles models has become feasible due to the advent of improved optimization methods (Cao, 2005).

Many dynamic model predictions however are affected by significant uncertainties, such as parametric uncertainties, disturbance noise, or state estimation errors. This may have an adverse effect on the control performance of the MPC and may lead to constraint violations. While the feedback introduced from the state update gives MPC some degree of robustness with regards to uncertainties, this is often not enough and hence explicit consideration of these uncertainties in the MPC formulation is crucial (Mesbah, 2016). Robust NMPC (RNMPC) assumes the uncertainties present to lie in a bounded set (Bemporad and Morari, 1999). RNMPC approaches include tube-based NMPC (Mayne et al., 2011) and min-max NMPC (Chen et al., 1997). These approaches allow guarantees on stability and performance in the worst-case realization of the uncertainties, which however may have a very small chance of occurrence and hence the solution may be overly conservative. Alternatively, stochastic NMPC (SNMPC) methods have been proposed, which assume the uncertainties to follow known probability density functions (pdf). Constraints and objective are formulated probabilistically. This allows for a pre-defined level of constraint violations in probability alleviating the issue of RNMPC by trading-off risk with closed-loop performance (Mesbah et al., 2014).

Several SNMPC approaches have been proposed. Assuming the uncertainties to have only finite number of realizations, multistage stochastic nonlinear programming approaches can be used to determine the exact solution (Lucia et al., 2013). Given this restriction, stochastic stability and recursive feasibility have been proven (Patrinos et al., 2014). For continuous stochastic uncertainties on the other hand it is difficult to propagate the uncertainties without being prohibitively expensive. An easy solution to this problem is given by successive linearization of the nonlinear dynamic system as in extended Kalman filter based NMPC (Lee and Ricker, 1994).

* Corresponding author.
E-mail address: eric.bradford@ntnu.no (E. Bradford).

https://doi.org/10.1016/j.compchemeng.2019.04.021
0098-1354/© 2019 Elsevier Ltd. All rights reserved.

In Bradford and Imsland (2018a) stochastic averaging is applied using the unscented transformation (UT). While both approaches are computationally cheap, they are only applicable to moderately nonlinear systems. In Sehr and Bitmead (2017) the particle filter equations are used to estimate the required statistics. This SNMPC algorithm however becomes quickly prohibitive in complexity due to the required number of samples. Similarly, in Maciejowski et al. (2007) Markov Chain MC is used instead with similar restrictions. In Alamir (2018) a supervised clustering algorithm is proposed to reduce the number of samples required to estimate the relevant statistical properties required, which however remains computationally expensive. For continuous-time dynamic systems Fokker–Planck equations have been used in Buehler et al. (2016) to propagate the pdfs of the uncertain variables. This approach is however quite expensive, since it requires the online solution of partial differential equations. In Weissel et al. (2009) it is proposed to use Gaussian mixtures for uncertainty propagation, in which most of the calculations are carried out offline. While this is generally quite efficient, it is only applicable for control actions from a discrete set and low dimensional systems. Alternatively, the statistics can be estimated using regression approaches such as polynomial chaos expansions (PCE) (Fagiano and Khammash, 2012) or Gaussian processes (Bradford and Imsland, 2018c). While these methods are considerably more efficient than MC sampling, they are only applicable for moderate dimensional problems due to exponential scaling with the number of uncertain parameters. In a similar fashion power series expansions (PSE) have been employed, which use a Taylor expansion of the dynamic system to propagate the uncertainties with similar advantages and disadvantages as using PCEs. While PSEs have been shown to have comparable accuracy to the PCE approach with the same polynomial order, it is difficult to extend to polynomial approximation of PSEs to orders higher than 2 (Kimaev and RicardezSandoval, 2017). Much of the work in SNMPC has been restricted to full state feedback with some exceptions. The UT work in Bradford and Imsland (2018a) uses the Unscented Kalman filter equations for state estimation, a probabilistic high-gain observer has been proposed in Homer and Mhaskar (2018) for state estimation in conjunction with a continuous-time SNMPC formulation, and lastly in Sehr and Bitmead (2017) particle filter equations were used for both propagation and state estimation.

In particular, PCE has received a lot of interest for SNMPC. PCEs are used to estimate the statistics online by building a stochastic surrogate model. This surrogate is then used in Fagiano and Khammash (2012) to approximate objective and constraints in expectation. The work was then further extended in Mesbah et al. (2014) to include chance constraints by using Chebychev's inequality. Streif et al. (2014) samples instead the PCE directly and approximates the chance constraints using the empirical distribution function, which is less conservative, but also computationally more expensive. PCE is often computationally too expensive for time-invariant uncertainties. The problem of time-varying additive noise (Bavdekar and Mesbah, 2016b) and time-varying nonadditive noise (Paulson and Mesbah, 2017) has been addressed by employing conditional probability rules. In Bradford and Imsland (2018b) feedback is considered in the control formulation using parametrized control policies to significantly lessen the conservativeness of the approach. PCE has also been used to great success for state estimation. Dutta and Bhattacharya (2010) use linear update rules considering higher-order moments. By sampling the PCE it can be updated directly using Bayes theorem as shown in Madankan et al. (2013). Similarly, Bavdekar and Mesbah (2016a) applies Bayes rule, however the approach accounts for time-varying additive disturbances and in addition uses the PCE for uncertainty propagation. In Bradford et al. (2019a) a PCE SNMPC algorithm was extended to the case of output feedback by using the state estimator proposed in Madankan et al. (2013), while in Bradford et al. (2019b) a similar approach is proposed considering in addition additive disturbance noise.

For batch processes we are often interested in constraints involving the end-product quality leading to a shrinking horizon NMPC (sh-NMPC) formulation, where the prediction horizon is equal to the final batch time. In Valappil and Georgakis (2002) a sh-NMPC algorithm using min-max successive linearization is proposed. Nagy and Braatz (2003) use an extended Kalman filter based sh-NMPC approach to account for parametric uncertainties and state estimation errors. The real-time implementation of a sh-NMPC for industrial applications is studied in Nagy et al. (2007). Mesbah et al. (2011) compares various optimization algorithms for sh-NMPC applied to a crystallization process. Nayhouse et al. (2015) employs a sh-NMPC algorithm to control the crystal growth and size distribution of ibuprofen. The multi-stage SNMPC algorithm has been extensively applied to batch processes (Lucia et al., 2013), while the PCE based SNMPC algorithms have been applied to sh-NMPC crystallization problems (Mesbah et al., 2014). In Rasoulian and Ricardez-Sandoval (2015) the evolution of a thin-film deposition process based on partial differential equations is controlled using a sh-NMPC implementation, for which the uncertainties are considered using PSEs.

In this paper we extend the previous work using a PCE based sh-SNMPC for batch processes (Bradford et al., 2019a; 2019b; Mesbah et al., 2014) in the output feedback case. PCEs are utilised, since for moderate dimensional problems these have been shown to give accurate estimates of the statistics required for relatively low number of samples compared to other sampling approaches (Lee and Chen, 2009). It was shown in Bradford and Imsland (2018b) that feedback needs to be included in the nonlinear PCE MPC formulation to not be overly conservative, which however has been otherwise ignored in such formulations. We propose to use time-invariant linear feedback gains to accomplish this, which are optimized over in addition to the open-loop control actions. The feedback only affects the predictions of the MPC, but are not themselves implemented outside of the MPC formulation. The parametric and state uncertainties are given by PCEs. It is assumed that at each sampling time only noisy output measurements are available, such that a nonlinear state estimator is used to update the PCE representations of the states and parameters. These representations are then efficiently exploited in the PCE based sh-SNMPC formulation to follow both path and end-point chance constraints to optimize an economic objective. The presence of time-varying additive disturbance noise is taken into account using the law of total expectation. The algorithm is verified on a challenging case study of a semi-batch reaction involving the production of the polymer polypropylene glycol. The aim is to directly minimize the required batch time subject to both safety and end-product constraints. The paper is comprised of the following sections. In Section 2 background information is given. In Section 3 a general problem definition is stated. In Section 4 the PCE state estimator is outlined, while in Section 5 we introduce the PCE sh-SNMPC formulation. Section 6 defines the algorithm using both the PCE state estimator and the PCE sh-SNMPC. Section 7 defines the case study to be solved, for which the results are shown and discussed in Section 8. Lastly, conclusions are given in Section 9.

2. Background

2.1. Introduction to polynomial chaos expansions

In this section we briefly outline PCEs specific for our purposes. For a more general review of PCEs, please refer to Xiu and Karniadakis (2003), Eldred and Burkardt (2009) and O'Hagan (2013). A PCE is a method to represent an arbitrary random variable γ with

finite second order moments as a function of random variables ξ with a known distribution. The random variable γ is expanded onto an orthogonal polynomial basis, which can be expressed as follows:

$$\gamma(\xi) = \sum_{\boldsymbol{\alpha}\in\mathbb{N}^{n_\xi}} a_{\boldsymbol{\alpha}}\phi_{\boldsymbol{\alpha}}(\xi) \tag{1}$$

where $\xi \in \mathbb{R}^{n_\xi}$ is called the *germ*, $\phi_{\boldsymbol{\alpha}} : \mathbb{R}^{n_\xi} \to \mathbb{R}$ are known multivariate polynomials comprising the basis with corresponding expansion coefficients $a_{\boldsymbol{\alpha}}$ and multidimensional summation indices $\boldsymbol{\alpha} \in \mathbb{N}^{n_\xi}$.

The probability distribution of the *germ* ξ is a modelling choice. Without loss of generality we assume ξ to follow a standard normal distribution with zero mean and unit variance, i.e. $\xi \sim \mathcal{N}(0, \mathbf{I})$. The multivariate polynomials in Eq. (1) are given as a tensor product of univariate polynomials of the components of ξ:

$$\phi_{\boldsymbol{\alpha}} = \prod_{i=1}^{n_\xi} \phi_{\alpha_i}(\xi_i) \tag{2}$$

where $\phi_{\alpha_i} : \mathbb{R} \to \mathbb{R}$ are univariate polynomials of ξ_i of order α_i. The multidimensional index $\boldsymbol{\alpha} = [\alpha_1, \ldots, \alpha_{n_\xi}]$ is hence used to define the degree of each univariate polynomial and the total order of the multivariate polynomial $\phi_{\boldsymbol{\alpha}}$ is consequently given as $|\boldsymbol{\alpha}| = \sum_{i=1}^{n_\xi} \alpha_i$.

The univariate polynomials ϕ_{α_i} are chosen to satisfy an orthogonality property according to the probability distribution of ξ_i, which in our case for standard normal distributions leads to Hermite polynomials:

$$\phi_{\alpha_i}(\xi_i) = (-1)^{\alpha_i} \exp\left(\frac{1}{2}\xi_i^2\right) \frac{d^{\alpha_i}}{d\xi_i^{\alpha_i}} \exp\left(-\frac{1}{2}\xi_i^2\right) \tag{3}$$

The multivariate polynomials built in this way according to Eqs. (2) and (3) have the following useful orthogonality property, which can be defined by the following inner product:

$$\begin{aligned}\langle \phi_{\boldsymbol{\alpha}}(\xi)\phi_{\boldsymbol{\beta}}(\xi)\rangle &= \mathbb{E}[\phi_{\boldsymbol{\alpha}}(\xi)\phi_{\boldsymbol{\beta}}(\xi)] = \int \phi_{\boldsymbol{\alpha}}(\xi)\phi_{\boldsymbol{\beta}}(\xi)p(\xi)d\xi \\ &= \tau_{\boldsymbol{\alpha}}^2 \delta_{\boldsymbol{\alpha}\boldsymbol{\beta}}\end{aligned} \tag{4}$$

where $p(\xi)$ is the pdf of ξ, $\delta_{\boldsymbol{\alpha}\boldsymbol{\beta}}$ is the Kronecker delta, i.e. $\delta_{\boldsymbol{\alpha}\boldsymbol{\beta}} = 1$ iff $\boldsymbol{\alpha} = \boldsymbol{\beta}$ otherwise $\delta_{\boldsymbol{\alpha}\boldsymbol{\beta}} = 0$. The normalization constant $\tau_{\boldsymbol{\alpha}}^2$ is dependent on the chosen family of polynomials and often known in practice.

Generally to use Eq. (1), it needs to be truncated. Keeping all terms up to a total order of m:

$$\gamma(\xi) \approx \sum_{0\le|\boldsymbol{\alpha}|\le m} a_{\boldsymbol{\alpha}}\phi_{\boldsymbol{\alpha}}(\xi) = \mathbf{a}^T\boldsymbol{\phi}(\xi) \tag{5}$$

where $\mathbf{a} \in \mathbb{R}^L$ and $\boldsymbol{\phi}(\xi) : \mathbb{R}^{n_\xi} \to \mathbb{R}^L$ are vectors of the coefficients and polynomials of the truncated expansion respectively. The truncated series consists of $L = \frac{(n_\xi+m)!}{n_\xi!m!}$ terms.

Often the coefficients $\mathbf{a}$ of the truncated PCE expansion in Eq. (5) are unknown and need to be determined using samples of γ. In this work we use the non-intrusive spectral projection approach based on the orthogonality property in Eq. (4) and the definition of the truncated series in Eq. (5):

$$a_j = \frac{\langle \gamma(\xi)\phi_{\boldsymbol{\alpha}_j}(\xi)\rangle}{\tau_{\boldsymbol{\alpha}_j}^2} = \frac{1}{\tau_{\boldsymbol{\alpha}_j}^2}\int \gamma(\xi)\phi_{\boldsymbol{\alpha}_j}(\xi)p(\xi)d\xi \tag{6}$$

where a_j refers to the jth coefficient of $\mathbf{a}$ with a corresponding $\boldsymbol{\alpha}_j$ multidimensional summation index.

The integral in Eq. (6) can be approximated using sampling. Quadrature methods are commonly used due to their improved convergence rates compared to crude MC. In the case of standard normal distributed germs Gauss-Hermite quadrature rules are employed, which approximate the integral in Eq. (6) as:

$$\int \gamma(\xi)\phi_{\boldsymbol{\alpha}_j}(\xi)p(\xi)d\xi \approx \sum_{q=1}^{N_q} w_q\gamma(\xi_q)\phi_{\boldsymbol{\alpha}_j}(\xi_q) \tag{7}$$

where N_q is the total number of quadrature points and ξ_q are the sample points with corresponding weights w_q given by the Gauss–Hermite quadrature rule.

This procedure leads to the following sample estimate $\hat{\mathbf{a}}$ of the coefficient vector $\mathbf{a}$:

$$\hat{\mathbf{a}} = (\mathbf{w}(\boldsymbol{\Gamma})^T\boldsymbol{\Phi}(\boldsymbol{\Xi}))^T * \boldsymbol{\tau}^{-2} \tag{8}$$

where $*$ denotes element-wise multiplication, $\boldsymbol{\Xi} = [\xi_1, \ldots, \xi_{N_q}]^T \in \mathbb{R}^{N_q\times n_\xi}$ represents the quadrature sample design, the response vector is given by $\boldsymbol{\Gamma} = [\gamma(\xi_1), \ldots, \gamma(\xi_{N_q})]^T \in \mathbb{R}^{N_q}$, $\mathbf{w}(\boldsymbol{\Gamma}) = [w_1\gamma(\xi_1), \ldots, w_{N_q}\gamma(\xi_{N_q})]^T \in \mathbb{R}^{N_q}$, $\boldsymbol{\tau}^{-2} = [\tau_{\boldsymbol{\alpha}_1}^{-2}, \ldots, \tau_{\boldsymbol{\alpha}_L}^{-2}]^T \in \mathbb{R}^L$ and $\boldsymbol{\Phi}(\boldsymbol{\Xi}) = [\boldsymbol{\phi}(\xi_1), \ldots, \boldsymbol{\phi}(\xi_{N_q})]^T \in \mathbb{R}^{N_q\times L}$.

So far we have limited ourselves to single dimensional random variable representations using PCEs, which can however easily be extended to multivariate random variables. Let a multivariate stochastic variable be given by $\boldsymbol{\gamma}(\xi) = [\gamma_1(\xi), \ldots, \gamma_{n_\gamma}(\xi)]^T \in \mathbb{R}^{n_\gamma=n_\xi}$ with coefficients collected in $\mathbf{A} = [\mathbf{a}_1, \ldots, \mathbf{a}_{n_\gamma}] \in \mathbb{R}^{L\times n_\xi}$, where we have assumed that each PCE is parametrized in terms of standard normal variables ξ with the same dimension as $\boldsymbol{\gamma}(\cdot)$. We further let each component of $\boldsymbol{\gamma}(\xi)$ be given by a truncated PCE with the same truncation order m and hence the same number of terms L.

Statistical moments are an important characterization of random variables. Assuming the multivariate random variable to be given by PCEs as defined above, the statistical moments are functions of the PCE coefficients $\mathbf{A}$ and can be defined as:

$$M_{\mathbf{r}}(\mathbf{A}) = \int \prod_{i=1}^{n_\xi} \gamma_i^{r_i}(\xi)p(\xi)d\xi \tag{9}$$

where $\mathbf{r} \in \mathbb{R}^{n_\xi}$ is a vector defining the moments with a total order $k = \sum_{i=1}^{n_\xi} r_i$.

Substituting the definition of the PCEs in Eq. (5) into Eq. (9) we arrive at (Dutta and Bhattacharya, 2010):

$$M_{\mathbf{r}}(\mathbf{A}) = \int \prod_{i=1}^{n_\xi} (\mathbf{a}_i^T\boldsymbol{\phi}(\xi))^{r_i}p(\xi)d\xi \tag{10}$$

Using Eq. (10) and the orthogonality property in Eq. (4) it can be shown that the mean values and covariances of $\boldsymbol{\gamma}$ are given by:

$$\mu^{\gamma_i} = \mathbb{E}[\gamma_i] = a_{i1} \tag{11}$$

$$\Sigma_{ij}^{\boldsymbol{\gamma}} = \mathbb{E}[(\gamma_i - \mu^{\gamma_i})(\gamma_j - \mu^{\gamma_j})] = \sum_{s=2}^{L}\sum_{t=2}^{L} a_{is}a_{jt}\langle \phi_{\boldsymbol{\alpha}_s}\phi_{\boldsymbol{\alpha}_t}\rangle \tag{12}$$

where μ^{γ_i} is the mean of γ_i and $\Sigma^{\boldsymbol{\gamma}}$ is the covariance matrix of $\boldsymbol{\gamma}$. Note that $\langle \phi_{\boldsymbol{\alpha}_s}\phi_{\boldsymbol{\alpha}_t}\rangle$ does not depend on the coefficients $\mathbf{a}$ and can hence be pre-computed. The diagonal of Eq. (12) define the variances of $\boldsymbol{\gamma}$.

2.2. Uncertainty propagation using PCEs

In this section we illustrate how PCEs can be used to efficiently propagate uncertainties through nonlinear functions using non-intrusive spectral projection as introduced in the previous section. Let an arbitrary nonlinear function $q(\cdot)$ of a random variable $\boldsymbol{\gamma}(\xi)$ be given by:

$$p = q(\boldsymbol{\gamma}(\xi)) \tag{13}$$

where ξ is the *germ* random variable parametrizing a random variable $\boldsymbol{\gamma}(\xi)$ as shown in the previous section.

The variable p is now a random variable as well parametrized by the *germ* ξ and the aim in this section is to determine its corresponding truncated PCE expansion. It should be noted that the PCE truncation order of p and $\gamma(\xi)$ can be dissimilar. To accomplish this we generate samples of ξ with corresponding weights using the Gauss-Hermite rule and evaluate p at those points. The PCE coefficients of p can then be determined using Eq. (8) as follows:

$$\hat{\mathbf{a}}_q = \mathbf{w}(\mathbf{\Gamma}_q)^T \mathbf{\Phi}(\mathbf{\Xi}) * \boldsymbol{\tau}^{-2} \tag{14}$$

where $\mathbf{w}(\mathbf{\Gamma}) = [w_1 q(\gamma(\xi_1)), \ldots, w_{N_q} q(\gamma(\xi_{N_q}))]^T$ with $\mathbf{\Gamma}_q = [q(\gamma(\xi_1)), \ldots, q(\gamma(\xi_{N_q})]^T$. The remaining terms are defined in Eq. (8).

Once the approximate coefficients $\hat{\mathbf{a}}_q$ have been determined, we can use Eqs. (11) and (12) to obtain mean and variance estimates for p as follows:

$$\mu^p = \mathbb{E}[p] \approx \hat{a}_{q1} \tag{15}$$

$$\sigma^p = \mathbb{E}[(p - \mathbb{E}[p])^2] \approx \sum_{s=2}^{L} \hat{a}_{qs}^2 \langle \phi_{\boldsymbol{\alpha}_s}^2 \rangle \tag{16}$$

From the above procedure only the response vector $\mathbf{\Gamma}_q$ and $\mathbf{w}(\mathbf{\Gamma}_q) = [w_1 q(\gamma(\xi_1)), \ldots, w_{N_q} q(\gamma(\xi_{N_q}))]^T$ depend on the values of p and hence the remaining terms can be pre-computed. We can therefore view this as a function for which a response vector $\mathbf{\Gamma}_q$ returns estimates of mean and variance of a nonlinear transformation, which we will denote as:

$$\mu^p \approx \mu_\zeta^{PCE}(\mathbf{\Gamma}_q) \tag{17}$$

$$\sigma^p \approx \sigma_\zeta^{PCE}(\mathbf{\Gamma}_q) \tag{18}$$

where $\zeta = \{m, \mathbf{w}, n_\xi, \mathbf{\Xi}\}$ is a collection of variables defining the mean and variance function, m is the total order of truncation of the PCE approximation of p, $\mathbf{w}$ is a vector of Gauss–Hermite weights, n_ξ the dimensionality of ξ, and $\mathbf{\Xi}$ is the sample design of ξ from the Gauss-Hermite rule.

Note that this approach to determine the statistics of p can be employed as long as clearly defined input-output data pairs are available utilising Eq. (16) to evaluate the required coefficients. A closed-form expression as shown in Eq. (13) is not necessarily required.

2.3. Laws of total expectation and total variance

PCEs are an efficient way to represent time-invariant probabilities, but become quickly prohibitive in complexity for time-varying uncertainties. This is because each instance of a time-varying uncertainty would require its own dimension in the germ distribution ξ, which scales exponentially with the number of terms L required in the PCE expansion, see Eq. (5). We therefore use the laws of total expectation and covariance to deal with the uncertainties in turn, i.e. using PCEs for the time-invariant uncertainties and utilising linearization for the time-varying uncertainties. In this section we introduce these laws.

Let γ and ω be arbitrary random variables and q an arbitrary function of these random variables, then according to the law of total expecation we have:

$$\mathbb{E}[q(\gamma, \omega)] = \mathbb{E}_\omega[\mathbb{E}_\gamma[q(\gamma, \omega)|\omega]] \tag{19}$$

The law of total variance can be stated as:

$$\begin{aligned}\mathrm{Var}[q(\gamma, \omega)] = {} & \mathbb{E}_\omega[\mathrm{Var}_\gamma[q(\gamma, \omega)|\omega]] \\ & + \mathrm{Var}_\omega[\mathbb{E}_\gamma[q(\gamma, \omega)|\omega]]\end{aligned} \tag{20}$$

Now we aim to use linearization to account for γ and PCE for ω to approximate the expectation and variance of $q(\gamma, \omega)$. Using linearization first we arrive at the following simplified expressions:

$$\mathbb{E}[q(\gamma, \omega)] \approx \mathbb{E}_\omega[q(\mu_\gamma, \omega)] \tag{21}$$

$$\mathrm{Var}[q(\gamma, \omega)] \approx \mathbb{E}_\omega[\mathbf{Q}(\omega)\mathbf{\Sigma}_\gamma \mathbf{Q}(\omega)^T] + \mathrm{Var}_\omega[\mathbb{E}_\gamma[q(\mu_\gamma, \omega)|\omega]] \tag{22}$$

where μ_γ is the mean of γ, $\mathbf{\Sigma}_\gamma$ denotes the covariance of γ and $\mathbf{Q}(\omega) = \frac{\partial q}{\partial \gamma}|_{\mu_\gamma, \omega}$ is the Jacobian of $q(\cdot)$ with respect to γ evaluated at μ_γ and ω.

Next using the PCE Eqs. (17) and (18) for ω we arrive at:

$$\mathbb{E}[q(\gamma, \omega)] \approx \mu_\zeta^{PCE}(\mathbf{\Gamma}_\mu^q) \tag{23}$$

$$\mathrm{Var}[q(\gamma, \omega)] \approx \mu_\zeta^{PCE}(\mathbf{\Gamma}_\sigma^q) + \sigma_\zeta^{PCE}(\mathbf{\Gamma}_\mu^q) \tag{24}$$

where $\mathbf{\Gamma}_\mu^q = [q(\mu_\gamma, \omega_1), \ldots, q(\mu_\gamma, \omega_{N_q})]$ and $\mathbf{\Gamma}_\sigma^q = [\mathbf{Q}(\omega_1)\mathbf{\Sigma}_\gamma \mathbf{Q}(\omega_1)^T, \ldots, \mathbf{Q}(\omega_{N_q})\mathbf{\Sigma}_\gamma \mathbf{Q}(\omega_{N_q})^T]$.

Here we have shown how two separate random variables ω and γ can be dealt with separately. In particular, regarding γ as time-varying it was accounted for using linearization, while assuming ω as time-invariant was considered using PCEs.

2.4. Chance constraint reformulation using Chebyshev's inequality

Let γ be a random variable, for which we have a chance constraint as follows:

$$\mathbb{P}(\gamma \leq 0) \geq 1 - \epsilon \tag{25}$$

Often the exact evaluation of Eq. (25) is difficult due to the integral definition of the probability function. Instead, we are however able to estimate the mean and variance of γ. Using Chebychev's inequality the probability constraints in Eq. (25) can be robustly transformed to the following equation (Mesbah et al., 2014):

$$\mu_\gamma + \kappa_\epsilon \sqrt{\sigma_\gamma} \leq 0 \tag{26}$$

where μ_γ and σ_γ are the mean and variance of γ respectively and $\kappa_\epsilon = \sqrt{\frac{1-\epsilon}{\epsilon}}$. Note the robust reformulation now only depends on the mean and variance of γ as required.

3. Problem definition

The dynamic system in this paper is assumed to be given by a discrete-time nonlinear equation system with stochastic parameters and additive disturbance noise:

$$\mathbf{x}_{t+1} = \mathbf{f}(\mathbf{x}_t, \mathbf{u}_t, \theta_t) + \mathbf{w}_t^{\mathbf{x}}, \quad \mathbf{x}_0 = \mathbf{x}_0(\xi) \tag{27}$$

$$\mathbf{y}_t = \mathbf{h}(\mathbf{x}_t, \theta_t) + \boldsymbol{\nu}_t \tag{28}$$

$$\theta_{t+1} = \theta_t + \mathbf{w}_t^{\theta}, \quad \theta_0 = \theta_0(\xi) \tag{29}$$

where t is the discrete time, $\mathbf{x} \in \mathbb{R}^{n_\mathbf{x}}$ are the system states, $\theta \in \mathbb{R}^{n_\theta}$ are parametric uncertainties, $\mathbf{u} \in \mathbb{R}^{n_\mathbf{u}}$ denote the control inputs, $\mathbf{f} : \mathbb{R}^{n_\mathbf{x}} \times \mathbb{R}^{n_\mathbf{u}} \times \mathbb{R}^{n_\theta} \to \mathbb{R}^{n_\mathbf{x}}$ represents the nonlinear dynamic system for the states, $\mathbf{y} \in \mathbb{R}^{n_\mathbf{y}}$ denote the measurements and $\mathbf{h} : \mathbb{R}^{n_\mathbf{x}} \times \mathbb{R}^{n_\theta} \to \mathbb{R}^{n_\mathbf{y}}$ are the output equations. Both the states $\mathbf{x}$ and the measurements $\mathbf{y}$ are assumed to be affected by normally distributed zero mean additive noise denoted by $\mathbf{w}^{\mathbf{x}}$ and $\boldsymbol{\nu}$ with known covariance matrices $\mathbf{\Sigma}_\nu$ and $\mathbf{\Sigma}_\mathbf{w}^\mathbf{x}$ respectively. In addition, the parametric uncertainties θ are also assumed to be affected by zero mean normally distributed additive disturbance noise to account for possible time variation denoted by $\mathbf{w}^\theta$ with corresponding covariance matrix $\mathbf{\Sigma}_\mathbf{w}^\theta$. The initial condition $\mathbf{x}_0$ and the initial parametric uncertainties θ_0 are assumed to follow PCEs

represented by $\mathbf{x}_0(\xi)$ and $\theta_0(\xi)$ respectively parametrized by $\xi \in \mathbb{R}^{n_\mathbf{x}+n_\theta} \sim \mathcal{N}(\mathbf{0}, \mathbf{I})$. For more information refer to Section 2.1. These PCEs express the initial uncertainty of θ and $\mathbf{x}$, which will usually represent a relatively broad distribution with large variances. Note by directly adding a disturbance term $\mathbf{d}_t \in \mathbb{R}^{n_\mathbf{x}}$ given by a PCE to Eq. (27), we could account for plant-model mismatch and update this mismatch using the filter introduced in Section 4.

In the following sections we will work with joint vectors of states and parametric uncertainties for simplification, which we will denote by $\mathbf{x}' = [\mathbf{x}, \theta]^T \in \mathbb{R}^{n_{\mathbf{x}'}=n_\mathbf{x}+n_\theta}$. The nonlinear equation system for $\mathbf{x}'$ can then be expressed as:

$$\mathbf{x}'_{t+1} = \mathbf{f}'(\mathbf{x}'_t, \mathbf{u}_t) + \mathbf{w}_t, \quad \mathbf{x}'_0 = \mathbf{x}'_0(\xi) \tag{30}$$

$$\mathbf{y}_t = \mathbf{h}(\mathbf{x}'_t) + \nu_t \tag{31}$$

where $\mathbf{f}'(\mathbf{x}'_t, \mathbf{u}_t) = [\mathbf{f}(\mathbf{x}'_t, \mathbf{u}_t), \theta_t]^T$, $\mathbf{w} = [\mathbf{w}^\mathbf{x}, \mathbf{w}^\theta]^T$ with corresponding covariance matrix $\mathbf{\Sigma}_\mathbf{w} = \text{diag}(\mathbf{\Sigma}^\mathbf{x}_\mathbf{w}, \mathbf{\Sigma}^\theta_\mathbf{w})$ and $\mathbf{x}'_0(\xi) = [\mathbf{x}_0(\xi), \theta_0(\xi)]^T$.

The aim in this paper is the development of an algorithm for the dynamic equation system stated above for batch processes. Generally the objective to be minimized depends on the properties of the final product at the end of the batch, such that the control problem commonly has a finite-horizon leading to a sh-NMPC formulation (Nagy and Braatz, 2003). We assume the objective to have the following form:

$$\begin{aligned} J(N, \mathbf{x}'_0(\xi), \mathbf{U}_N) &= \mathbb{E}[J^d(N, \mathbf{x}'_0(\xi), \mathbf{U}_N)], \quad J^d(N, \mathbf{x}'_0(\xi), \mathbf{U}_N) \\ &= \mathcal{M}(\mathbf{x}'_N) + \sum_{t=0}^{N-1} \mathcal{L}(\mathbf{x}'_t, \mathbf{u}_t) \end{aligned} \tag{32}$$

where N is the time horizon, $\mathcal{M} : \mathbb{R}^{n_{\mathbf{x}'}} \to \mathbb{R}$ is the Mayer term, $\mathcal{L} : \mathbb{R}^{n_{\mathbf{x}'} \times n_\mathbf{u}} \to \mathbb{R}$ is the Lagrange term, and $\mathbf{U}_N = [\mathbf{u}_0, \ldots, \mathbf{u}_{N-1}] \in \mathbb{R}^{n_\mathbf{u} \times N}$ are the control actions that need to be determined.

The objective is taken as the expectation of a nonlinear function with a Mayer and Lagrange term, i.e. the objective is to minimize the expected value of $J^d(N, \mathbf{x}'_0(\xi, \mathbf{U}_N)$ given the initial PCE $\mathbf{x}'_0(\xi)$ and the dynamic system stated in Eqs. (30) and (31).

The minimization of the objective is subject to both the adherence of path constraints and terminal constraints. The control inputs are subject to hard constraints expressed by the set $\mathbb{U}$. For batch processes common path constraints are safety limits on the reactor temperature and terminal constraints are commonly a minimum product quality to be reached. The constraints can be stated as follows:

$$\mathbb{P}[g_j(\mathbf{x}'_t, \mathbf{u}_t) \leq 0] \geq 1 - \epsilon \quad \forall (t, j) \in \{1, \ldots, N\} \times \{1, \ldots, n_g\} \tag{33}$$

$$\mathbb{P}[g^N_j(\mathbf{x}'_N) \leq 0] \geq 1 - \epsilon \quad \forall j \in \{1, \ldots, n^N_g\} \tag{34}$$

$$\mathbf{u}_t \in \mathbb{U} \quad \forall t \in \{0, \ldots, N-1\} \tag{35}$$

where $g_j : \mathbb{R}^{n_{\mathbf{x}'} \times n_\mathbf{u}} \to \mathbb{R}$ are the path constraint functions, $g^N_j : \mathbb{R}^{n_{\mathbf{x}'}} \to \mathbb{R}$ are the terminal constraint functions and ϵ is the probability of constraint violation.

The constraints are given as so-called chance-constraints due to the presence of the stochastic uncertainties in both the initial condition $\mathbf{x}'_0$ and the disturbance noise. Each constraint in Eqs. (33) and (34) should be violated at most by a low probability of ϵ despite the stochastic uncertainties present to maintain feasibility.

4. Polynomial chaos expansion state estimation

In this section we introduce a nonlinear state estimator to update a prior probability distribution of the state $\mathbf{x}'$ given by a PCE using the available measurements from Eq. (28). The nonlinear filter is similar to the one given in Madankan et al. (2013) and Mühlpfordt et al. (2016), however these works do not consider additive disturbance noise. We assume we are at sampling time t and wish to update the PCE representation of the uncertainties given the newly available measurements. Let $D_t = \{\mathbf{y}_1 \ldots, \mathbf{y}_t\}$ be the available measurements up to time t. In particular Bayes' rule is used recursively for the update of $\mathbf{x}'$ using D_t:

$$p(\mathbf{x}'_t|D_t) = \frac{p(\mathbf{x}'_t|D_{t-1})p(\mathbf{y}_t|\mathbf{x}'_t, D_{t-1})}{p(\mathbf{y}_t|D_{t-1})} \tag{36}$$

For convenience we denote $\mathcal{N}(\gamma|\mu_\gamma, \mathbf{\Sigma}_\gamma)$ as the normal probability density of a random variable γ with mean $\boldsymbol{\mu}_\gamma$ and covariance $\mathbf{\Sigma}_\gamma$:

$$\mathcal{N}(\gamma|\boldsymbol{\mu}_\gamma, \mathbf{\Sigma}_\gamma) = \det(2\pi\,\mathbf{\Sigma}_\gamma)^{-\frac{1}{2}} \exp\left(-\frac{1}{2}(\gamma - \mu_\gamma)^T \mathbf{\Sigma}^{-1}_\gamma (\gamma - \mu_\gamma)\right) \tag{37}$$

The terms on the RHS of Eq. (36) are dependent on the dynamic system introduced in Section 3 and are defined below in turn.

4.1. $p(\mathbf{x}'_t|D_{t-1})$

Prior distribution of $\mathbf{x}'_t$ given the previous measurements D_{t-1}, which can be expressed as:

$$p(\mathbf{x}'_t|D_{t-1}) = \int p(\mathbf{x}'_t|\mathbf{x}'_{t-1})p(\mathbf{x}'_{t-1}|D_{t-1})d\mathbf{x}'_{t-1} \tag{38}$$

where $p(\mathbf{x}'_t|\mathbf{x}'_{t-1}) = \mathcal{N}(\mathbf{x}'_t|\mathbf{f}'(\mathbf{x}'_{t-1}, \mathbf{u}_{t-1}), \mathbf{\Sigma}_\mathbf{w})$ is a multivariate normal pdf with mean given by the dynamics defined in Eq. (27) and the covariance by the disturbance noise evaluated at $\mathbf{x}'_t$. It should be noted that without disturbance noise $p(\mathbf{x}'_t|D_{t-1}) = \int \delta(\mathbf{x}'_t - \mathbf{f}'(\mathbf{x}'_{t-1}, \mathbf{u}_{t-1}))p(\mathbf{x}'_{t-1}|D_{t-1})d\mathbf{x}'_{t-1}$.

4.2. $p(\mathbf{y}_t|\mathbf{x}'_t, D_{t-1})$

The pdf of the current measurement $\mathbf{y}_t$ given $\mathbf{x}'_t$, which can be stated as follows:

$$p(\mathbf{y}_t|\mathbf{x}'_t, D_{t-1}) = \mathcal{N}(\mathbf{y}_t|\mathbf{h}(\mathbf{x}'_t), \mathbf{\Sigma}_\nu) \tag{39}$$

4.3. $p(\mathbf{y}_t|D_{t-1})$

Total probability of observation $\mathbf{y}_t$ given previous measurements can be expressed as:

$$p(\mathbf{y}_t|D_{t-1}) = \int p(\mathbf{y}_t|\mathbf{x}'_t, D_{t-1})p(\mathbf{x}'_t|D_{t-1})d\mathbf{x}'_t \tag{40}$$

If we take both sides of Eq. (36) times $\prod_{j=1}^{n_\xi}(x'_{tj})^{r_j}$ and integrate over both sides with respect to $\mathbf{x}'_t$ we obtain:

$$M^+_\mathbf{r} = \frac{\int \prod_{j=1}^{n_\xi}(x'_{tj})^{r_j} p(\mathbf{y}_t|\mathbf{x}'_t, D_{t-1})p(\mathbf{x}'_t|D_{t-1})d\mathbf{x}'_t}{p(\mathbf{y}_t|D_{t-1})} \tag{41}$$

where from Eq. (36) $M^+_\mathbf{r} = \int \prod_{j=1}^{n_\xi}(x'_{tj})^{r_j} p(\mathbf{x}'_t|D_t)d\mathbf{x}'_t$ and $k = \sum_{j=1}^{n_\xi} r_j$. Now by definition $M^+_\mathbf{r}$ refers to the various kth order moments of the updated distribution of $\mathbf{x}'_t$, $p(\mathbf{x}'_t|D_t)$.

In our case the uncertainties of $\mathbf{x}'_t$ are given by PCEs, which we have so far not taken advantage of. Let $\mathbf{x}'_{t-1}(\xi)$ refer to the previously estimated PCEs of $\mathbf{x}'_t$ using the measurements up to time $t-1$, i.e. $\mathbf{x}'_{t-1}(\xi)$ refers to $\mathbf{x}'_{t-1}|D_{t-1}$. The RHS of Eq. (41) is approximated using sampling. The probability distribution $\mathbf{x}'_{t-1}(\xi)$ is readily sampled by generating samples of ξ, which is known to follow a standard normal distribution. In addition, we also require

samples of the disturbance $\mathbf{w}$ to estimate the integral in Eq. (38). In this work we used Latin hypercube sampling with the inverse normal cumulative transformation, which has an improved convergence over crude MC, see Stein (1987) for more information. The sample approximation of the total probability in Eq. (40) can be stated as:

$$\alpha = \frac{1}{N_s^{SE}} \sum_{s=1}^{N_s^{SE}} \mathcal{N}(\mathbf{y}_t | \mathbf{h}(\mathbf{x}_t'^{(s)}), \mathbf{\Sigma}_\nu) \tag{42}$$

where α is the sample estimate of $p(\mathbf{y}_t|D_{t-1})$, $\mathbf{x}_t'^{(s)} = \mathbf{f}(\mathbf{x}_{t-1}(\xi_s), \mathbf{u}_{t-1}) + \mathbf{w}_s$, N_s^{SE} is the sample size, $\xi_s \sim \mathcal{N}(\mathbf{0}, \mathbf{I})$, and $\mathbf{w}_s \sim \mathcal{N}(\mathbf{0}, \mathbf{\Sigma_w})$ are the sample points.

Using the sample estimate in Eq. (42) and applying a further sample estimate to Eq. (41) we obtain:

$$M_{\mathbf{r}}^{(s)+} = \frac{\sum_{s=1}^{N_s^{SE}} \prod_{j=1}^{n_\xi} (x_{tj}'^{(s)})^{r_j} \mathcal{N}(\mathbf{y}_t | \mathbf{h}(\mathbf{x}_t'^{(s)}), \mathbf{\Sigma}_\nu)}{\alpha N_s^{SE}} \tag{43}$$

where $M_{\mathbf{r}}^{(s)+}$ is an approximation of the RHS of Eq. (41).

To update $\mathbf{x}_{t-1}'(\xi)$ to $\mathbf{x}_t'(\xi)$ we match the moments defined in Eq. (43) with those of the PCE $\mathbf{x}_t'(\xi)$, which are a function of its coefficients as shown in Eq. (10). The PCE is then fitted by solving a nonlinear least-squares optimization problem:

$$\hat{\mathbf{A}}_t = \arg\min_{\mathbf{A}_t} \sum_{k \le m^{SE}} ||M_{\mathbf{r}}^{+}(\mathbf{A}_t) - M_{\mathbf{r}}^{(s)+}||_2^2 \tag{44}$$

where $k = \sum_{j=1}^{n_\xi} r_j$ was defined above as the order of the moments and hence m^{SE} defines the total order of moments we aim to match. $M_{\mathbf{r}}^{+}(\mathbf{A}_t)$ is parametrized by $\mathbf{A}_t$ as shown in Eq. (10). The estimated coefficients $\hat{\mathbf{A}}_t$ then define the updated PCE $\mathbf{x}_t'(\xi)$ as required, which approximately represents the probability distribution of $\mathbf{x}_t'|D_t$. The overall procedure to update an initial PCE expansion $\mathbf{x}_{t-1}'(\xi)$ to $\mathbf{x}_t'(\xi)$ is summarised in Algorithm 1 below.

Algorithm 1 PCE state estimation

Input : $\mathbf{y}_t$, $\mathbf{f}'(\mathbf{x}', \mathbf{u})$, $\mathbf{h}(\mathbf{x}')$, $\mathbf{\Sigma}_\nu$, $\mathbf{\Sigma_w}$, $\mathbf{x}_{t-1}'(\xi)$, m^{SE}, N_s^{SE}

1. Generate N_s^{SE} Gaussian distributed Latin hypercube samples of ξ and $\mathbf{w}$.
2. Using these samples approximate α in Eq. 42.
3. Using the samples and α approximate the moments with an order of m^{SE} or less in Eq. 43.
4. Solve the optimization problem in Eq. 44 to obtain the updated coefficients that yield $\mathbf{x}_t'(\xi)$.

Output : $\mathbf{x}_t'(\xi)$

5. Polynomial chaos expansion model predictive control

In this section we introduce the PCE based sh-SNMPC formulation used to solve the problem defined in Section 3 using the dynamic equation system for the joint state vector in Eqs. (30) and (31). We assume we are at sampling time t and we are given a current PCE approximation of $\mathbf{x}_t'|D_t$ denoted by $\mathbf{x}_t'(\xi)$ from the PCE state estimator, which accounts for our current uncertainty of the initial condition given the available measurements, see Section 4. To approximate the chance constraints and the objective it is not only necessary to propagate the uncertainty of the initial condition $\mathbf{x}_t'(\xi)$, but also the uncertainty of the additive disturbance noise.

5.1. Control policy parametrization

A common issue of MPC under uncertainty is the fact that open-loop uncertainties grow unboundedly leading to control actions that are exceedingly conservative, since the feedback through the state update is disregarded. Eventually the OCP will become infeasible with a large enough prediction horizon (Yan and Bitmead, 2005). Therefore, to ensure reasonable predictions of the uncertainty feedback needs to be incorporated in the optimal control formulation. Optimization over general causal feedback policies is however often intractable (Bertsekas, 2011), such that the optimization is restricted over a class of parametrized feedback policies (Goulart et al., 2006). In this paper we employ the following parametrization of the control input:

$$\mathbf{u}_k = \mathbf{v}_k + \mathbf{K}(\mathbf{y}_k - \mu_{\mathbf{y},\mathbf{k}}) \tag{45}$$

where $\mathbf{v}_k \in \mathbb{R}^{n_\mathbf{u}}$ are the mean of the applied control inputs, $\mathbf{K} \in \mathbb{R}^{n_\mathbf{u} \times n_\mathbf{y}}$ are linear time-invariant feedback gains and $\mu_{\mathbf{y},\mathbf{k}}$ denotes the mean of $\mathbf{y}_k$.

This is a relatively common form to parametrize the control policy, where $\mathbf{v}_k$ corresponds to the control inputs of the nominal system, whereas $\mathbf{K}$ is times by the difference of the real system outputs to the nominal system outputs for correction. This control parametrization is for example used in Nagy and Braatz (2004) to design a linear feedback gain for batch processes. The importance to account for feedback is highlighted in Fig. 1. A stochastic OCP was solved twice once optimizing over a linear time-invariant feedback gain in addition to the open-loop control actions shown on the left-hand side and once over only the open-loop control actions shown on the right-hand side subject to an adiabatic temperature constraint. As can be seen on the left-hand side the adiabatic temperature trajectories are considerably narrower than on the right-hand side and hence accounting for feedback leads to a considerably less conservative OCP solution.

5.2. Uncertainty propagation

For the uncertainty propagation in the sh-SNMPC formulation we use the results in Sections 2.2–2.3. In this section we outline recursive equations to obtain the required mean and variances of the objective, constraints and outputs from an initial time t to a final shrinking time horizon N^{sh} to formulate the MPC problem. The uncertainty represented by the PCE $\mathbf{x}_t'(\xi)$ is accounted for using the PCE Eqs. (17) and (18), while the additive disturbance noise from the states and measurements are considered using linearization. The overall mean and variance of the objective and chance constraints are then determined using the laws of total expectation and variance as shown in Section 2.3.

Let $\mu_{\mathbf{x}',k}(\xi)$ correspond to the mean and $\mathbf{\Sigma}_{\mathbf{x}',k}(\xi)$ to the covariance of $\mathbf{x}_k'$ given ξ, defined as:

$$\mu_{\mathbf{x}',k}(\xi) = \mathbb{E}[\mathbf{x}_k'|\xi] \tag{46}$$

$$\Sigma_{\mathbf{x}',k_{ij}}(\xi) = \mathbb{E}\Big[(\mathbf{x}_{ki}' - \mathbb{E}[\mathbf{x}_{ki}'])(\mathbf{x}_{kj}' - \mathbb{E}[\mathbf{x}_{kj}'])|\xi\Big] \tag{47}$$

We propagate the uncertainty of $\mu_{\mathbf{x}',k}(\xi)$ and $\mathbf{\Sigma}_{\mathbf{x}',k}(\xi)$ from the additive disturbances using linearization for the dynamic equation system in Eqs. (30) and (31), which yields:

$$\mu_{\mathbf{x}',k+1}(\xi) = \mathbf{f}'(\mu_{\mathbf{x}',k}(\xi), \mu_{\mathbf{u}_k}(\xi)), \ \mu_{\mathbf{x}',0}(\xi) = \mathbf{x}_t'(\xi) \tag{48}$$

$$\begin{aligned}\mathbf{\Sigma}_{\mathbf{x}',k+1}(\xi) &= \mathbf{A}_k(\xi)\mathbf{\Sigma}_{\mathbf{x}',k}(\xi)\mathbf{A}_k(\xi)^T + \mathbf{B}_k(\xi)\mathbf{\Sigma}_{\mathbf{u},k}(\xi)\mathbf{B}(\xi)^T \\ &\quad + 2\mathbf{A}_k(\xi)\mathbf{\Sigma}_{\mathbf{x'u},k}(\xi)\mathbf{B}_k(\xi)^T, \ \mathbf{\Sigma}_{\mathbf{x}',0}(\xi) = \mathbf{0}\end{aligned} \tag{49}$$

where $\mathbf{A}_k(\xi) = \frac{\partial \mathbf{f}'}{\partial \mathbf{x}'}|_{\mu_{\mathbf{x}',k}(\xi), \mu_{\mathbf{u}_k}(\xi)}$, and $\mathbf{B}_k(\xi) = \frac{\partial \mathbf{f}'}{\partial \mathbf{u}}|_{\mu_{\mathbf{x}',k}(\xi), \mu_{\mathbf{u}_k}(\xi)}$ are Jacobian matrices of $\mathbf{f}'(\mathbf{x}', \mathbf{u})$ with respect to $\mathbf{x}'$ and $\mathbf{u}$ respectively

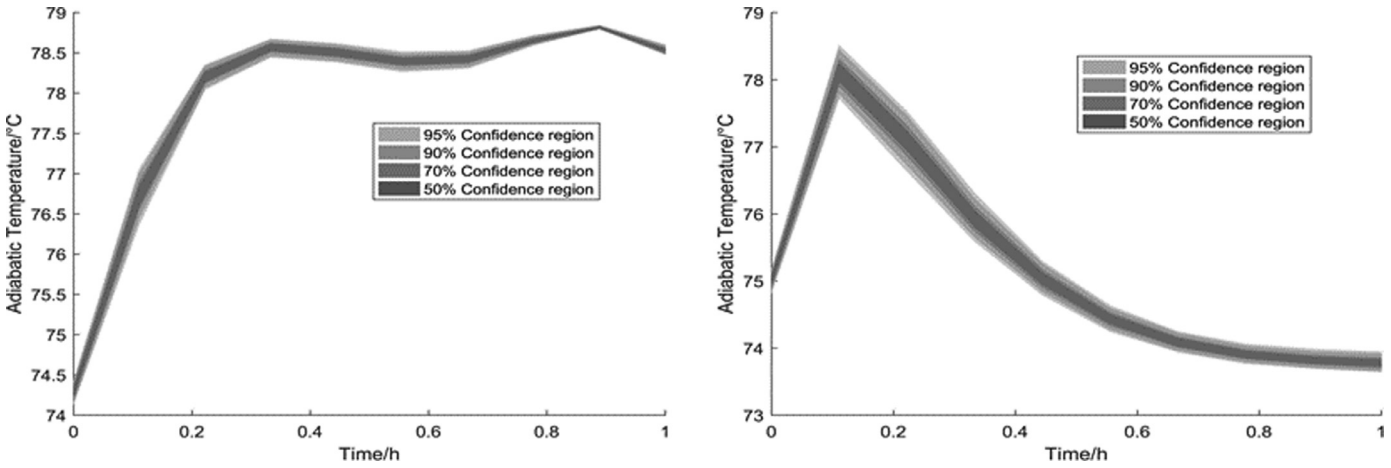

Fig. 1. OCP adiabatic temperature trajectories accounting for linear time-invariant feedback on the left-hand side and not accounting for feedback on the right-hand side.

evaluated at $\mathbf{x}' = \mu_{\mathbf{x}',k}(\xi)$ and $\mathbf{u} = \mu_{\mathbf{u}_k}(\xi) = \mathbf{v}_k + \mathbf{K}(\mathbf{h}(\mu_{\mathbf{x}',k}(\xi)) - \mu_{\mathbf{y}_k})$. Let each component of $\mu_{\mathbf{y}_k}$ be given by $\mu_{\mathbf{y}_{ki}} = \mu_{\zeta}^{PCE}(\mathbf{\Gamma}_{\mu,k}^{y_{ki}})$, which is defined later in Eq. (61).

For the control policy parametrization in Eq. (45) the covariance matrices $\mathbf{\Sigma}_{\mathbf{u},k}(\xi)$ and $\mathbf{\Sigma}_{\mathbf{x}'\mathbf{u},k}(\xi)$ can be expressed as:

$$\mathbf{\Sigma}_{\mathbf{u},k}(\xi) = \mathbf{K}\Big(\mathbf{H}_k(\xi)\mathbf{\Sigma}_{\mathbf{x}',k}(\xi)\mathbf{H}_k(\xi)^T + \mathbf{\Sigma}_{\nu}\Big)\mathbf{K}^T \tag{50}$$

$$\mathbf{\Sigma}_{\mathbf{x}'\mathbf{u},k}(\xi) = \mathbf{\Sigma}_{\mathbf{x}',k}(\xi)\mathbf{H}_k(\xi)^T\mathbf{K}^T \tag{51}$$

where $\mathbf{H}_k(\xi) = \frac{\partial \mathbf{h}}{\partial \mathbf{x}'}|_{\mu_{\mathbf{x}',k}(\xi)}$ is the Jacobian matrix of $\mathbf{h}(\mathbf{x}')$ evaluated at $\mathbf{x}' = \mu_{\mathbf{x}',k}(\xi)$.

From Eq. (48) we obtain $\mu_{\mathbf{x}',k}(\xi)$ recursively for all $k \in \{1,\dots,N^{sh}\}$, while Eq. (49) gives us $\mathbf{\Sigma}_{\mathbf{x}',k}(\xi)$ recursively for all $k \in \{1,\dots,N^{sh}\}$. The objective, output measurements, and constraint functions are however assumed to be nonlinear functions of these, see Section 3. We therefore require further simplification to estimate the required statistics to formulate the SNMPC problem. Using further linearization these quantities can be determined as follows:

$$\mathbb{E}[J^d(N^{sh}, \mathbf{x}_t'(\xi), \mathbf{U}_{N^{sh}})|\xi] \approx J^d(N^{sh}, \mathbf{x}_t'(\xi), \mathbf{U}_{N^{sh}}) \tag{52}$$

$$\mathbb{E}[g_j(\mathbf{x}_k', \mathbf{u}_k)|\xi] \approx g_j(\mu_{\mathbf{x}',k}(\xi), \mu_{\mathbf{u}_k}(\xi)) \tag{53}$$

$$\mathbb{E}[g_j^N(\mathbf{x}_{N^{sh}}')|\xi] \approx g_j^N(\mu_{\mathbf{x}',N^{sh}}(\xi)) \tag{54}$$

$$\mathbb{E}[\mathbf{y}_k|\xi] \approx \mathbf{h}(\mu_{\mathbf{x}',k}(\xi)) \tag{55}$$

$$\mathrm{Var}[g_j(\mathbf{x}_k', \mathbf{u}_k)|\xi] \approx \mathbf{G}_{j_k}(\xi)\mathbf{\Sigma}_{\mathbf{x}',k}(\xi)\mathbf{G}_{j_k}(\xi)^T \tag{56}$$

$$\mathrm{Var}[g_j^{N^{sh}}(\mathbf{x}_{N^{sh}}')|\xi] \approx \mathbf{G}_j^N(\xi)\mathbf{\Sigma}_{\mathbf{x}',N^{sh}}(\xi)\mathbf{G}_j^N(\xi)^T \tag{57}$$

where $\mathbf{G}_{j_k}(\xi) = \frac{\partial \mathbf{g}_j}{\partial \mathbf{x}'}|_{\mu_{\mathbf{x}',k}(\xi),\mu_{\mathbf{u}_k}(\xi)}$ is the Jacobian matrix of $\mathbf{g}_j(\mathbf{x}', \mathbf{u})$ evaluated at $\mathbf{x}' = \mu_{\mathbf{x}',k}(\xi)$ and $\mathbf{u} = \mu_{\mathbf{u}_k}(\xi)$ and $\mathbf{G}_j^N(\xi) = \frac{\partial \mathbf{g}_j^N}{\partial \mathbf{x}'}|_{\mu_{\mathbf{x}',N^{sh}}(\xi)}$ is the Jacobian matrix of $\mathbf{g}_j^N$ evaluated at $\mathbf{x}' = \mu_{\mathbf{x}',N^{sh}}(\xi)$.

We now have the means and variances of the objective, constraint functions and outputs accounting for the additive disturbance noise, but ignoring the uncertainty from the initial condition $\mathbf{x}_t'(\xi)$. As highlighted the means and variances, and their respective terms are all functions of $\mathbf{x}_t'(\xi)$ and in turn of ξ on which they are conditioned. To obtain the overall means and variances required we use the laws of total expectation and variance as shown in Section 2.3. This is accomplished by creating a Gauss-Hermite sample design of ξ, which we will denote as $\mathbf{\Xi} = [\xi_1,\dots,\xi_{N_q}]$ with N_q quadrature points. Obtaining the respective response vectors $\mathbf{\Gamma}$ for the conditional means and variances in Eqs. (52)–(57) for these samples and applying the PCE mean and variance estimates from Section 2.2, the overall variances and expectations are given by:

$$\mathbb{E}[J^d(N^{sh}, \mathbf{x}_t'(\xi), \mathbf{U}_{N^{sh}})] \approx \mu_{\zeta_{\mathrm{NMPC}}}^{PCE}(\mathbf{\Gamma}_{\mu}^{J^d}) \tag{58}$$

$$\mathbb{E}[g_j(\mathbf{x}_k', \mathbf{u}_k)] \approx \mu_{\zeta_{\mathrm{NMPC}}}^{PCE}(\mathbf{\Gamma}_{\mu,k}^{g_j}) \tag{59}$$

$$\mathbb{E}[g_j^N(\mathbf{x}_{N^{sh}}')] \approx \mu_{\zeta_{\mathrm{NMPC}}}^{PCE}(\mathbf{\Gamma}_{\mu}^{g_j^N}) \tag{60}$$

$$\mathbb{E}[y_{ki}] \approx \mu_{\zeta_{\mathrm{NMPC}}}^{PCE}(\mathbf{\Gamma}_{\mu,k}^{y_{ki}}) \tag{61}$$

$$\mathrm{Var}[g_j(\mathbf{x}_k', \mathbf{u}_k)] \approx \mu_{\zeta_{\mathrm{NMPC}}}^{PCE}(\mathbf{\Gamma}_{\sigma,k}^{g_j}) + \sigma_{\zeta_{\mathrm{NMPC}}}^{PCE}(\mathbf{\Gamma}_{\mu,k}^{g_j}) \tag{62}$$

$$\mathrm{Var}[g_j^N(\mathbf{x}_{N^{sh}}')] \approx \mu_{\zeta_{\mathrm{NMPC}}}^{PCE}(\mathbf{\Gamma}_{\sigma}^{g_j^N}) + \sigma_{\zeta_{\mathrm{NMPC}}}^{PCE}(\mathbf{\Gamma}_{\mu}^{g_j^N}) \tag{63}$$

where $\mathbf{\Gamma}_{\mu,k}^{y_{ki}} = [\mathbf{h}(\mu_{\mathbf{x}',k}(\xi_1)),\dots,\mathbf{h}(\mu_{\mathbf{x}',k}(\xi_{N_q}))]$,

$\mathbf{\Gamma}_{\mu}^{J^d} = [J^d(N^{sh}, \mathbf{x}_t'(\xi_1), \mathbf{U}_{N^{sh}}),\dots,J^d(N^{sh}, \mathbf{x}_t'(\xi_{N_q}), \mathbf{U}_{N^{sh}})]^T$,

$\mathbf{\Gamma}_{\mu,k}^{g_j} = [g_j(\mu_{\mathbf{x}',k}(\xi_1), \mu_{\mathbf{u}_k}(\xi_1)),\dots,g_j(\mu_{\mathbf{x}',k}(\xi_{N_q}), \mu_{\mathbf{u}_k}(\xi_{N_q}))]$,

$\mathbf{\Gamma}_{\mu}^{g_j^N} = [g_j^N(\mu_{\mathbf{x}',N^{sh}}(\xi_1)),\dots,g_j^N(\mu_{\mathbf{x}',N^{sh}}(\xi_{N_q}))]$,

$\mathbf{\Gamma}_{\sigma,k}^{g_j} = [\mathbf{G}_{j_k}(\xi)\mathbf{\Sigma}_{\mathbf{x}',k}(\xi_1)\mathbf{G}_{j_k}(\xi_1)^T,\dots,\mathbf{G}_{j_k}(\xi)\mathbf{\Sigma}_{\mathbf{x}',k}(\xi_{N_q})\mathbf{G}_{j_k}(\xi_{N_q})^T]$

and

$\mathbf{\Gamma}_{\sigma}^{g_j^N} = [\mathbf{G}_j^N(\xi_1)\mathbf{\Sigma}_{\mathbf{x}',N^{sh}}(\xi_1)\mathbf{G}_j^N(\xi)^T,\dots,\mathbf{G}_j^N(\xi)\mathbf{\Sigma}_{\mathbf{x}',N^{sh}}(\xi_{N_q})\mathbf{G}_j^N(\xi_{N_q})^T]$.

Note that each sample of ξ corresponds to a separate initial condition and hence a separate nonlinear equation system given by Eq. (30). In essence the PCE methodology generates separate samples of the initial condition, which each correspond to a distinctive nonlinear dynamic system that are propagated individually together with their linearized variance approximations. From these samples the overall means and variances are then determined from the coefficients of the PCE expansion as shown in Sections 5.2 and 2.3. $\zeta_{\mathrm{NMPC}} = \{m_{\mathrm{NMPC}}, \mathbf{w}_{\mathrm{NMPC}}, n_{\xi} = n_{\mathbf{x}'}, \mathbf{\Xi}_{\mathrm{NMPC}}\}$ defines in this context the variables of the PCE mean and variance function, see Section 5.2, which are the order of truncation of the PCE approximation, the Gauss-Hermite weights, the dimensionality of n_{ξ} given by the number of states and uncertain parameters, and lastly the Gaussian-Hermite sample design. Next we formulate the sh-SNMPC problem based on the above equations.

5.3. Chance constraint reformulation

In Section 5.2 we show how to obtain estimates of the mean and variance of the objective and constraint functions. While this is sufficient to approximate the objective defined in Section 3, we still require estimates for the chance constraints defined in Eqs. (33) and (34). In Section 2.4 it was shown how Chebyshev's inequality can be used to robustly reformulate chance constraints exploiting only mean and variance of the constrained variable, which leads to the following robust reformulations of Eqs. (33) and (34) using the estimates of mean and variances given in Eqs. (59)–(63):

$$\mu^{PCE}_{\zeta_{\text{NMPC}}}(\mathbf{\Gamma}^{g_j}_{\mu,k}) + \kappa_\epsilon \sqrt{\mu^{PCE}_{\zeta_{\text{NMPC}}}(\mathbf{\Gamma}^{g_j}_{\sigma,k}) + \sigma^{PCE}_{\zeta_{\text{NMPC}}}(\mathbf{\Gamma}^{g_j}_{\mu,k})} \leq 0 \tag{64}$$

$$\mu^{PCE}_{\zeta_{\text{NMPC}}}(\mathbf{\Gamma}^{g^N_j}_{\mu}) + \kappa_\epsilon \sqrt{\mu^{PCE}_{\zeta_{\text{NMPC}}}(\mathbf{\Gamma}^{g^N_j}_{\sigma}) + \sigma^{PCE}_{\zeta_{\text{NMPC}}}(\mathbf{\Gamma}^{g^N_j}_{\mu})} \leq 0 \tag{65}$$

where $\kappa_\epsilon = \sqrt{\frac{1-\epsilon}{\epsilon}}$.

5.4. Stochastic nonlinear optimal control formulation

In this section we formulate the stochastic optimal control problem to be solved in a shrinking horizon fashion at each sampling time t given a probability distribution of the initial condition represented by its PCE $\mathbf{x}'_t(\xi)$ and the dynamic equation system defined in Section 3. The formulation is based on the propagation equations outlined in Section 5.2 and the reformulations of the chance constraints in Section 5.3. We optimize over both open-loop control actions $\mathbf{v}_k$ and a time-invariant feedback control gain $\mathbf{K}$ to account for feedback. The overall formulation can be stated as follows:

$$\begin{aligned}
&\underset{\mathbf{V}_{N^{sh}},\mathbf{K}}{\text{minimize}} \quad \mu^{PCE}_{\zeta_{\text{NMPC}}}(\mathbf{\Gamma}^{J^d}_{\mu}) \\
&\text{subject to} \\
&\mu^{PCE}_{\zeta_{\text{NMPC}}}(\mathbf{\Gamma}^{g_j}_{\mu,k}) + \kappa_\epsilon \sqrt{\mu^{PCE}_{\zeta_{\text{NMPC}}}(\mathbf{\Gamma}^{g_j}_{\sigma,k}) + \sigma^{PCE}_{\zeta_{\text{NMPC}}}(\mathbf{\Gamma}^{g_j}_{\mu,k})} \leq 0 \\
&\mu^{PCE}_{\zeta_{\text{NMPC}}}(\mathbf{\Gamma}^{g^N_j}_{\mu}) + \kappa_\epsilon \sqrt{\mu^{PCE}_{\zeta_{\text{NMPC}}}(\mathbf{\Gamma}^{g^N_j}_{\sigma}) + \sigma^{PCE}_{\zeta_{\text{NMPC}}}(\mathbf{\Gamma}^{g^N_j}_{\mu})} \leq 0 \\
&\mu_{\mathbf{u}_k}(\xi_i) = \mathbf{v}_k + \mathbf{K}(\mathbf{h}(\mu_{\mathbf{x}',k}(\xi_i)) - \mu_{\mathbf{y}_k}) \in \mathbb{U} \\
&\mu^{(i)}_{\mathbf{x}',0} = \mathbf{x}'_t(\xi_i) \\
&\forall (k,j) \in \{1,\dots,N^{sh}\} \times \{1,\dots,n_g\} \\
&\forall j \in \{1,\dots,n^N_g\} \\
&\forall k \in \{0,\dots,N^{sh}-1\} \\
&\forall i \in \{1,\dots,N_q\}
\end{aligned} \tag{66}$$

where $\mathbf{V}_{N^{sh}} = [\mathbf{v}_0,\dots,\mathbf{v}_{N^{sh}-1}]^T$ is a matrix of open-loop control actions. It should be noted that the initial control input is given by $\mathbf{v}_0$, which is the output of the MPC algorithm. The initial measurement is known and hence feedback does not apply for the first control action in the problem above, i.e. $\mathbf{h}(\mu_{\mathbf{x}',k}(\xi_i)) = \mu_{\mathbf{y}_0} \forall i \in \{1,\dots,N_q\}$. The linear feedback gain $\mathbf{K}$ is only used to lead to more realistic future predictions.

6. Algorithm

In this section we state the algorithm to solve the problem defined in Section 3. Initially at time $t = 0$ we are given a probability distribution represented by a PCE of $\mathbf{x}'$ denoted by $\mathbf{x}'_0(\xi)$. In addition, we define the DAE system to be controlled by $\mathbf{f}(\mathbf{x}', \mathbf{u})$ and their measurement equation $\mathbf{h}(\mathbf{x}')$, and the corresponding additive disturbances defined by the covariance matrices $\mathbf{\Sigma}_\nu$ and $\mathbf{\Sigma}_\mathbf{w}$. The overall time horizon N needs to be given, which is also equal to the number of control inputs. Further, we define the objective $J^d(N, \mathbf{x}'_0(\xi), \mathbf{u}_N)$ with path $g_j(\mathbf{x}'_t, \mathbf{u}_t)$ and terminal constraints $g^N_j(\mathbf{x}'_N)$ with a corresponding chance of constraint violation ϵ given an overall time horizon of N. We define m_{SE} and N^{SE}_s as the order to be matched in the state estimator, while N^{SE}_s denotes the number of samples to approximate the moments in the state estimator, see Algorithm 1 in Section 4. Lastly, ζ_{NMPC} is required to define the PCE approximation of the sh-SNMPC in Section 5. Overall we suggest to represent the states $\mathbf{x}'$ at each sampling time t using PCEs introduced in Section 2.1. The SNMPC algorithm exploits this uncertainty description to control the dynamic system in Section 3. The available measurements are utilised to update the PCE representation recursive as outlined in Section 4. The overall algorithm is given below as Algorithm 2.

Algorithm 2 Output feedback PCE sh-SNMPC

Input : $\mathbf{f}'(\mathbf{x}', \mathbf{u})$, $\mathbf{h}(\mathbf{x}')$, $\mathbf{\Sigma}_\nu$, $\mathbf{\Sigma}_\mathbf{w}$, $\mathbf{x}'_0(\xi)$, m_{SE}, N^{SE}_s, N, ζ_{NMPC}
Initialize: $N^{sh} := N$
for *each sampling time* $t = 0, 1, 2, \dots, N-1$ **do**
1. Solve the PCE SNMPC problem in Eq. 66 with $\mathbf{x}'_t(\xi)$ and time horizon N^{sh}.
2. Apply the first optimal control action $\mathbf{v}_0$ to the plant.
3. Measure $\mathbf{y}_{t+1}$.
4. Apply PCE filter to update $\mathbf{x}'_t(\xi)$ to $\mathbf{x}'_{t+1}(\xi)$ using $\mathbf{y}_{t+1}$.
5. Set $N^{sh} := N^{sh} - 1$.

end

7. Case study

The algorithm outlined in Section 6 is applied to a challenging polymerization semi-batch reactor case study. The reactor produces the polymer polypropylene glycol from the monomer propylene oxide (PO). A schematic of the process is shown below in Fig. 2.

7.1. Semi-batch reactor model

A complex model for this process has been proposed in Nie et al. (2013a), which uses a separate balance equation for each

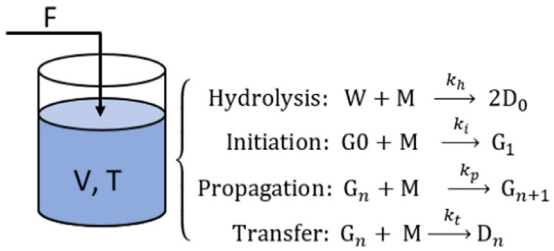

Fig. 2. F is the monomer feedrate, V and T are the volume and temperature of the liquid in the reactor respectively, W is water, M is the monomer, D$_n$ and G$_n$ are the dormant and active product chains with length n respectively.

Table 1
Parameter values for dynamic model defined in Eqs. (67) and (68) taken from Nie et al. (2013a).

Parameter	Value	Units	Description
MW_{PO}	58.08	kg/kmol	Molecular weight of PO
ΔH_p	−92048	kJ/kmol	Enthalpy of reaction for propagation reaction
A_t	950410	m^3/kmol/s	Pre-exponential factor of transfer kinetic constant
E_{Ap}	69172	kJ/kmol	Activation energy of propagation reaction
E_{At}	105018	kJ/kmol	Activation energy of transfer reaction
n_C	2.0	kmol	Amount of catalyst
R	8.314	kJ/kmol/K	Universal gas constant
γ_0	10	kmol	Zeroth polymer moment (Methanol)

specific chain length. This model was employed in Jung et al. (2015) for crude NMPC and in Jang et al. (2016) for multi-stage robust NMPC. The computational times reported were approximately in the range of 30 s to minutes, which is relatively high and can be attributed to the relative complexity of the dynamic model in Nie et al. (2013a). In particular the high dimensionality of the state would cause issues with the proposed methodology due to the scaling of PCEs, see Section 2.1. To reduce the dimensionality and complexity of the model we therefore applied the so-called "method of moments" (Nie et al., 2013b). This leads to balance equations describing the moments of the polymer as opposed to the concentration of each specific chain length, which is commonly sufficient to estimate key performance indicators. Further, we disregard the balance equations for the unsaturated polymer chain length and in addition assume that there are only trace amounts of water or methanol present. This means that hydrolysis only takes place in negligible amounts and hence can be ignored. In the original dynamic model perfect temperature control was assumed. Due to the relative importance of temperature control with regards to safety, we added an energy balance. The modified ordinary differential equation system consists of 4 balance equations and can be stated as follows:

$$\dot{m} = FMW_{PO} \qquad m(0) = m_0(\xi) \tag{67a}$$

$$\dot{T} = \frac{(-\Delta H_p)k_p n_C PO}{V m C_{pb}} - \frac{UA(T - T_C)}{mC_{pb}} - \frac{FMW_{PO}C_{pf}(T - T_f)}{mC_{pb}} \qquad T(0) = T_0(\xi) \tag{67b}$$

$$\dot{PO} = F - \frac{n_C(k_p + k_t)PO}{V} \qquad PO(0) = PO_0(\xi) \tag{67c}$$

$$\dot{\gamma}_1 = \frac{k_p n_C PO}{V} \qquad \gamma_1(0) = \gamma_{10}(\xi) \tag{67d}$$

where m is the liquid mass in the reactor in [kg], F is the feed rate of the monomer in [kmol/s], T is the temperature of the reactor in [K], PO is the amount of monomer in [kmol] and γ_1 is the first moment and hence the average molecular weight of the polymer chains in [kmol], MW_{PO} is the molecular weight of PO in [kg/kmol], ΔH_p is the enthalpy of the propagation reaction in [kJ/kmol], k_p is the kinetic constant of the propagation equation in [m^3/kmol/s], n_C is the amount of catalyst in [kmol], V is the volume of the liquid in the reactor in m^3, C_{pb} and C_{pf} are the heat capacities of the bulk liquid and the monomer feed respectively in [kJ/kg/K], k_t is the transfer kinetic constant in [m^3/kmol/s], T_C is the cooling water temperature in [K] and UA is the overall heat transfer coefficient in [kJ/K].

The kinetic constants are given by Arrhenius equations as functions of temperature, while the heat capacities C_{pb} and C_{pf} are also functions of temperature Nie et al. (2013a):

$$k_p = A_p \exp(-E_{Ap}/RT) \tag{68a}$$

$$k_t = A_t \exp(-E_{At}/RT) \tag{68b}$$

$$C_{pf} = 0.92 + 8.871 \times 10^{-3}T - 3.1 \times 10^{-5}T^2 + 4.78 \times 10^{-8}T^3 \tag{68c}$$

$$C_{pb} = 1.1 + 2.72 \times 10^{-3}T \tag{68d}$$

Two parameters in the above model are assumed to be uncertain: A_p and UA. The remaining values of parameters to define Eqs. (67) and (68) are given in Table 1. Note that for the assumptions made the amount of the zeroth polymer moment γ_0 in the reactor is fixed, since no hydrolysis takes place.

The control inputs are given by the monomer feed rate F and the cooling water temperature T_C. In compact form we can write $\mathbf{x} = [m, T, PO, \gamma_1]^T$, $\mathbf{u} = [F, T_C]^T$ and $\theta = [A_p, UA]^T$. The corresponding joint vector is then given by $\mathbf{x}' = [m, T, PO, \gamma_1, A_p, UA]^T$. The continuous-time dynamic system we denote by $\tilde{\mathbf{f}}'(\mathbf{x}', \mathbf{u}) = [\dot{m}, \dot{T}, \dot{PO}, \dot{\gamma}_1, 0, 0]^T$.

We assume that reactor temperature T and the amount of monomer PO are measured at each sampling time with $\mathbf{y} = [T, PO]^T$. The measurement equation $\mathbf{h}(\cdot)$ is given as follows:

$$\mathbf{h}(\mathbf{x}') = [T, PO]^T \tag{69}$$

The initial uncertainty of the states $\mathbf{x}$ and the uncertain parameters θ is given by their respective initial PCEs, which are defined as:

$$m_0(\xi) = 1538 \tag{70a}$$

$$PO_0(\xi) = 10 + \xi_2 \tag{70b}$$

$$T_0(\xi) = 378.15 + 4\xi_3 \tag{70c}$$

$$\gamma_{10}(\xi) = 10 + 0.5\xi_4 \tag{70d}$$

$$A_{P0}(\xi) = 10 + \xi_5 \tag{70e}$$

$$UA_0(\xi) = 15 + 4\xi_6 \tag{70f}$$

The overall initial PCE is now given by $\mathbf{x}'_0(\xi) = [m_0(\xi), PO_0(\xi), T_0(\xi), \gamma_{10}(\xi), A_{P0}(\xi), UA_0(\xi)]^T$. The PCEs of $\mathbf{x}'$ given by $\mathbf{x}'(\xi)$ have a truncation order of 2.

The additive disturbance and measurement noise is defined by their respective covariance matrices, which were set to:

$$\mathbf{\Sigma_w} = \mathrm{diag}(1, 10^{-3}, 1, 2.5 \times 10^{-1}, 5 \times 10^{-2}, 2 \times 10^{-1}) \tag{71}$$

$$\mathbf{\Sigma_\nu} = \mathrm{diag}(0.25, 1 \times 10^{-3}) \tag{72}$$

7.2. Problem set-up

The time horizon N was set to 8 with a variable continuous time of t_{batch}. Given the dynamic system in Eq. (67) we define the objective and constraints in this section to define a problem as the one given in Section 3. The control algorithm aims to minimize the required batch time t_{batch} with a penalty on the control change, which can be stated as follows:

$$J^d(N, \mathbf{x}'_0(\xi), \mathbf{U}_N) = t_{\text{batch}} + \sum_{k=1}^{N} \mathbf{\Delta}_{\mathbf{u}_k}^T \mathbf{R} \mathbf{\Delta}_{\mathbf{u}_k} \tag{73}$$

where $\mathbf{\Delta}_{\mathbf{u}_k} = \mathbf{u}_k - \mathbf{u}_{k-1}$ and $\mathbf{R} = \text{diag}(10^{-6}, 10^{-4})$.

The batch time is defined to describe the discrete-time equation for a control horizon N:

$$\mathbf{x}'_{t+1} = \int_0^{t_{\text{batch}}/N} \bar{\mathbf{f}}'(\mathbf{x}'_t, \mathbf{u}_t) dt + \mathbf{x}'_t \tag{74}$$

The minimum of the objective above is subject to two terminal constraints and a path constraint. The path constraint aims to keep the reactor temperature to remain below 420K for safety reasons:

$$g(\mathbf{x}'_t, \mathbf{u}_t) = T - 420 \leq 0 \tag{75}$$

The two terminal constraints are given by two product quality constraints. Firstly, the batch needs to reach a specified number average molecular weight ($NAMW$) in [kg/mol] of 350 defined as $NAMW = MW_{\text{PO}} \frac{\gamma_1}{\gamma_0}$. Secondly, the amount of monomer PO in the final batch may not exceed 1000ppm. The two end-point product quality constraint can consequently be stated as:

$$g_1^N(\mathbf{x}'_N) = -MW_{\text{PO}} \frac{\gamma_1}{\gamma_0} + 350 \leq 0 \tag{76}$$

$$g_2^N(\mathbf{x}'_N) = 10^6 \times \left(\frac{POMW_{\text{PO}}}{m} \right) - 1000 \leq 0 \tag{77}$$

The chance of constraint violation was set to $\epsilon = 0.05$ for the constraints defined above. The monomer feed rate and the cooling water temperature were constrained as follows:

$$0 \leq F \leq 0.01 \tag{78}$$

$$298.15 \leq T_C \leq 423.15 \tag{79}$$

7.3. Solution approach

To solve the case study we need to discretize the continuous-time equation system outlined in Eq. (67) to obtain the required discrete-time equation used in the problem definition in Section 3. For the discredization we applied orthogonal Radau collocation (Biegler, 2010). Each control interval is modelled by one polynomial with an overall degree of 5. Further, we require linearization matrices for the states and control inputs for the discrete time system to propagate the additive disturbance noise as outlined in Section 5.2, which are given as follows (Kristoffersen and Holden, 2017):

$$\mathbf{A}_k(\xi) = \exp\left(\frac{\partial \bar{\mathbf{f}}'}{\partial \mathbf{x}'} \Big|_{\mathbf{x}' = \mu_{\mathbf{x}',k}(\xi), \mathbf{u}_k = \mu_{\mathbf{u}_k}(\xi)} \right) \tag{80a}$$

$$\mathbf{B}_k(\xi) = \left(\frac{\partial \bar{\mathbf{f}}'}{\partial \mathbf{x}'} \Big|_{\mathbf{x}' = \mu_{\mathbf{x}',k}(\xi), \mathbf{u}_k = \mu_{\mathbf{u}_k}(\xi)} \right)^{-1} (\mathbf{A}_k(\xi) - \mathbf{I}) \times \left(\frac{\partial \bar{\mathbf{f}}'}{\partial \mathbf{u}} \Big|_{\mathbf{x}' = \mu_{\mathbf{x}',k}(\xi), \mathbf{u}_k = \mu_{\mathbf{u}_k}(\xi)} \right) \tag{80b}$$

The resulting optimization problems for both the PCE sh-SNMPC problem and the PCE state estimator were solved using Casadi (Andersson et al., 2018) to obtain the gradients of the problem using automatic differentiation in conjuncation with IPOPT (Wächter and Biegler, 2006). The "real" plant model was simulated using IDAS (Hindmarsh et al., 2005). The PCE state estimator aims to match up to 3 orders with overall 10,000 samples to estimate the posterior moments, i.e. $m_{SE} = 3$ and $N_s^{SE} = 10000$. For the Gauss-Hermite samples we use a sparse rule for the weights $\mathbf{w}$ and sample design $\mathbf{\Xi}$ as outlined in (Jia et al., 2012) with a polynomial accuracy of 3. The PCE of the sh-SNMPC has a truncation order of 2 with a dimensionality of ξ of 6 corresponding to the dimensionality of $\mathbf{x}'$. The parameters for the PCE sh-SNMPC algorithm are then given by $\zeta_{\text{NMPC}} = [2, \mathbf{w}, 6, \mathbf{\Xi}]$.

8. Results and discussions

In this section we present and discuss the results of the case study outlined in the previous section. For comparison purposes we compare three different sh-NMPC variations, which are as follows:

- SNMPC with feedback: The algorithm as outlined in Section 6 optimizing over both a linear feedback gain and open-loop control actions.
- SNMPC without feedback: The algorithm as outlined in Section 6, but optimizing over only open-loop control actions and setting the linear feedback gain to zero.
- Nominal NMPC: A NMPC algorithm based on the same dynamic model and discredization with the state estimate equal to the best-estimate given by the mean of the PCE state estimator. Objective and constraints are deterministic in this case with soft constraints used for feasibility.

The sh-SNMPC variations were each run for the economic MPC problem minimizing the objective given in Eq. (73) subject to the safety path constraint in Eq. (75), and end-point product quality constraints defined in Eqs. (76) and (77). Note that the time-invariant feedback gain is never actually implemented, since the first control action does not depend on it, see the SNMPC formulation in Eq. (66). Instead, this inclusion of feedback only serves to obtain more realistic and less conservative predictions. The actual closed-loop response depends on the feedback from the state update.

8.1. Example scenario

We first run the three sh-NMPC variations on a single scenario, where we set the initial condition to the following: $\mathbf{x}'_0 = [m_0, P0_0, T_0, \gamma_{10}, A_{P0}, UA_0]^T = [1538, 9.0, 385, 9.5, 7.5, 10]^T$. This can be seen as a single realization of the initial PCE stated in Eq. (70). The results of this are summarised in Figs. 3–11. In Figs. 3–6 the trajectories of the four states are shown for each algorithm with the corresponding state estimate. In addition an error-bar is shown corresponding to a 95% confidence interval of the state estimate. In Figs. 7 and 8 the two control inputs are shown respectively for each algorithm. Fig. 9 shows the sampling times for each algorithm, which is minimized for the objective and changes at each sampling interval due to the improved estimates of the uncertain parameters and states. Lastly, Figs. 10 and 11 illustrate the evolution of the uncertain parameter probability density functions for the "SNMPC with feedback" variation. We can draw the following conclusions from the graphs depicted:

- Fig. 5 shows the relative conservativeness of the SNMPC without feedback compared to the nominal NMPC and the SNMPC with feedback. While the latter two algorithms lead to trajectories that quickly approach the temperature constraint, the SNMPC without feedback first drastically reduces the temperature

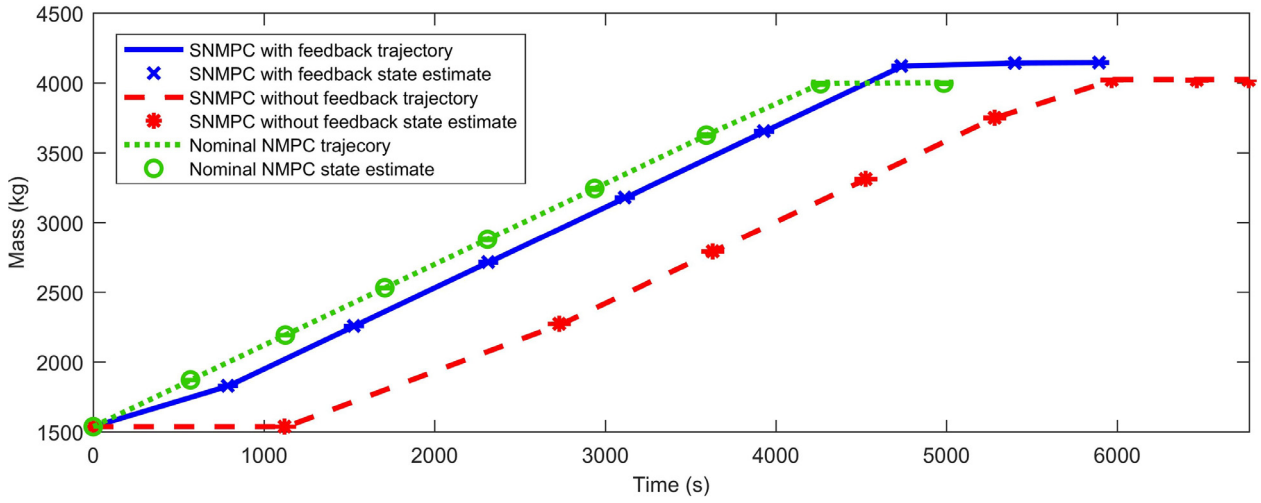

Fig. 3. Scenario trajectories of the reactor mass for each algorithm variation.

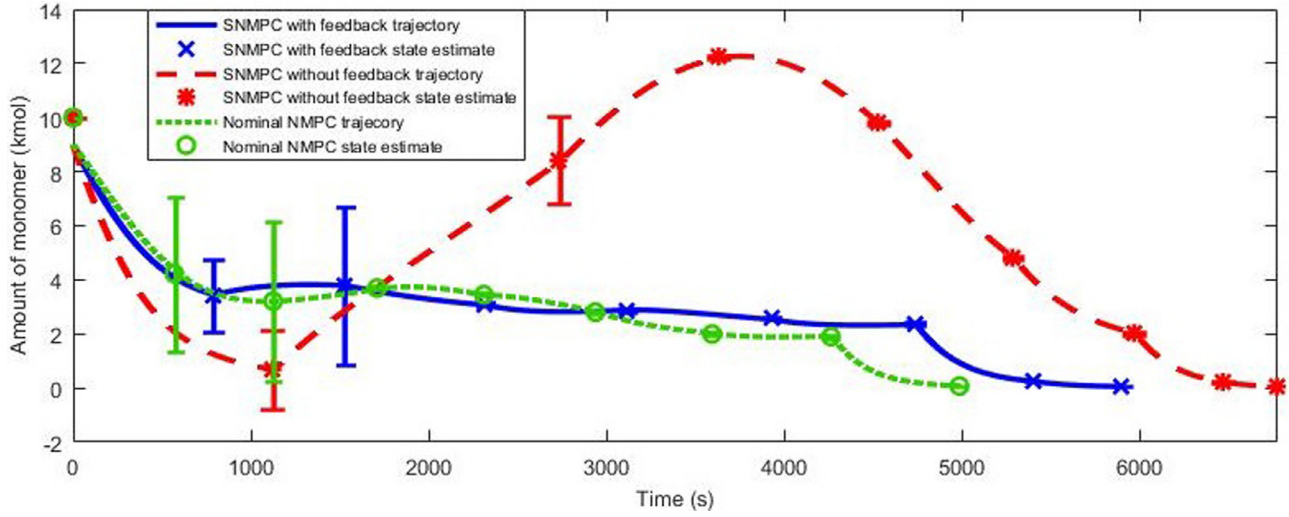

Fig. 4. Scenario trajectories of the amount of monomer for each algorithm variation.

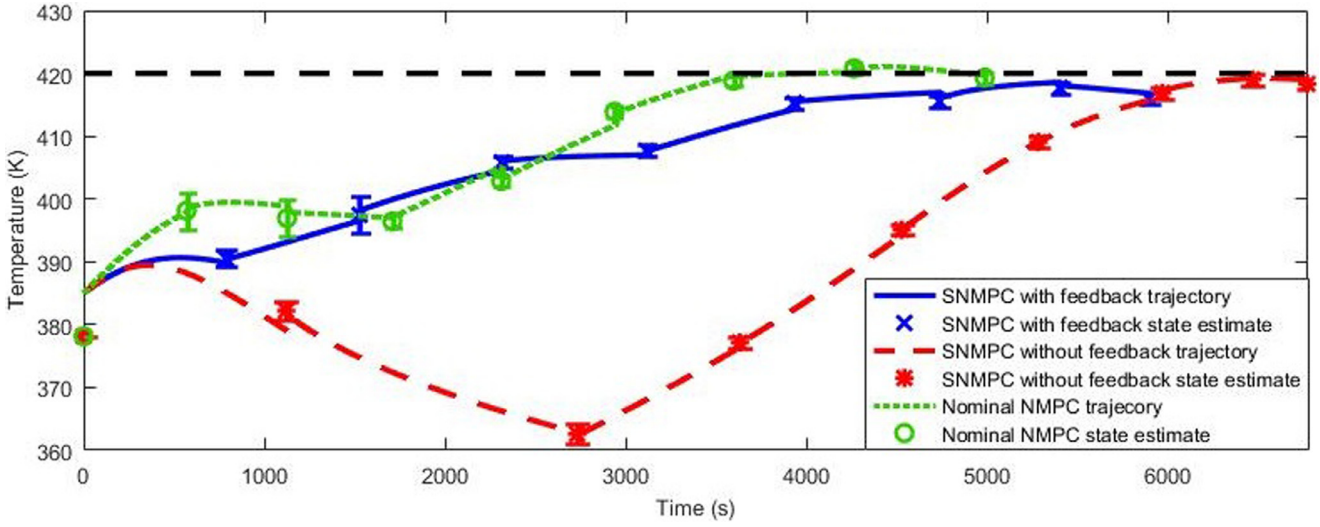

Fig. 5. Scenario trajectories of the reactor temperature for each algorithm variation.

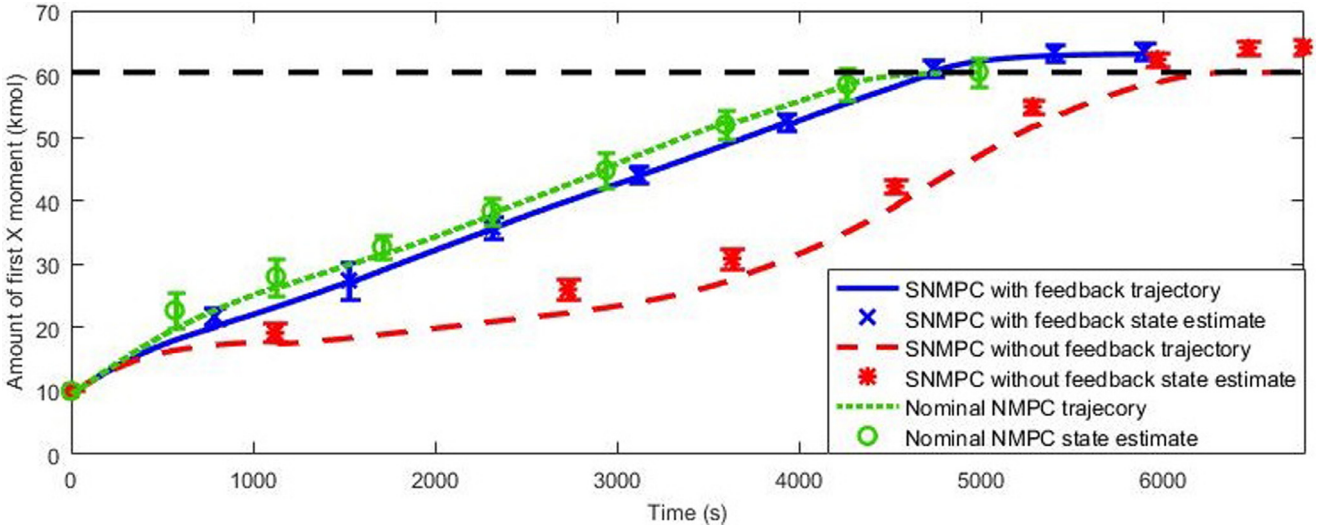

Fig. 6. Scenario trajectories of the first polymer moment for each algorithm variation.

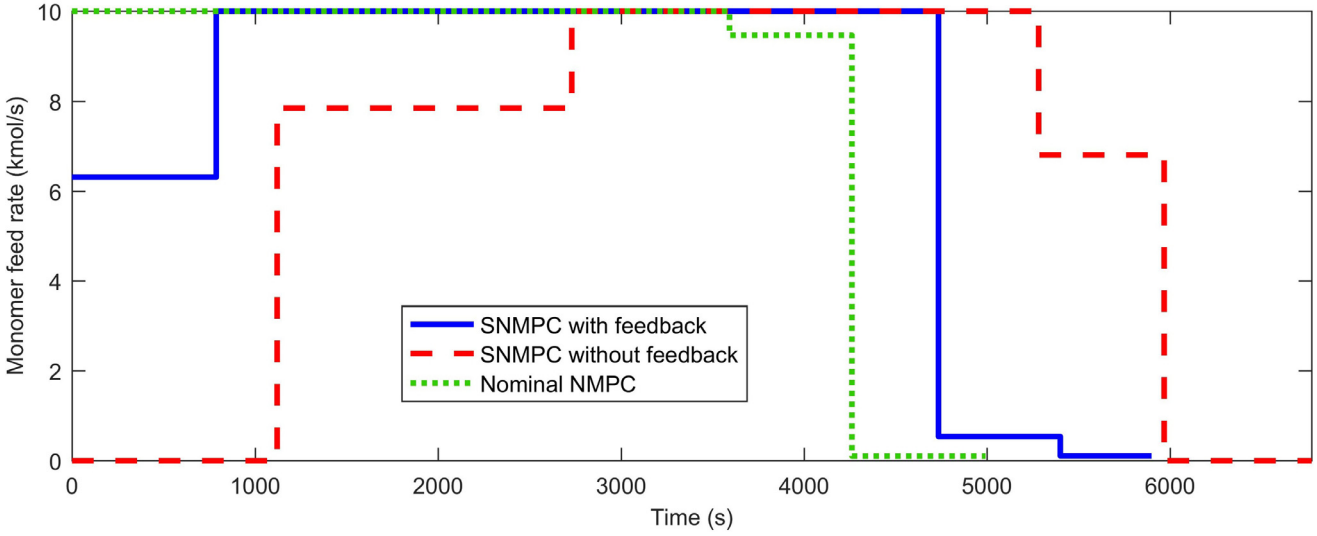

Fig. 7. Monomer feed rate trajectory for each algorithm variation.

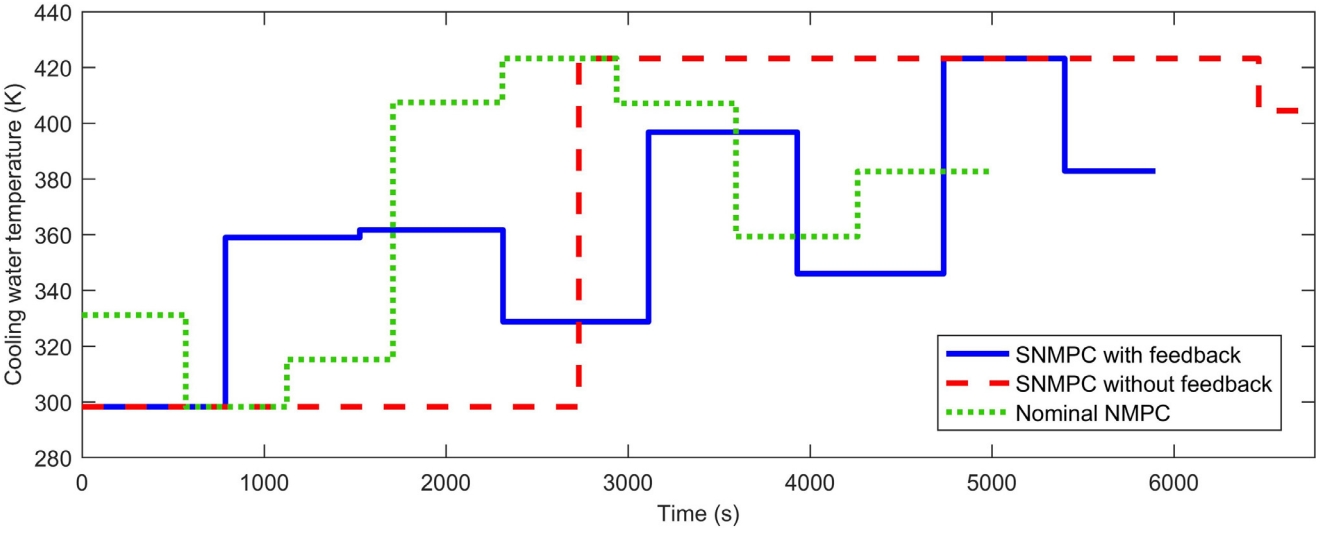

Fig. 8. Cooling temperature trajectory for each algorithm variation.

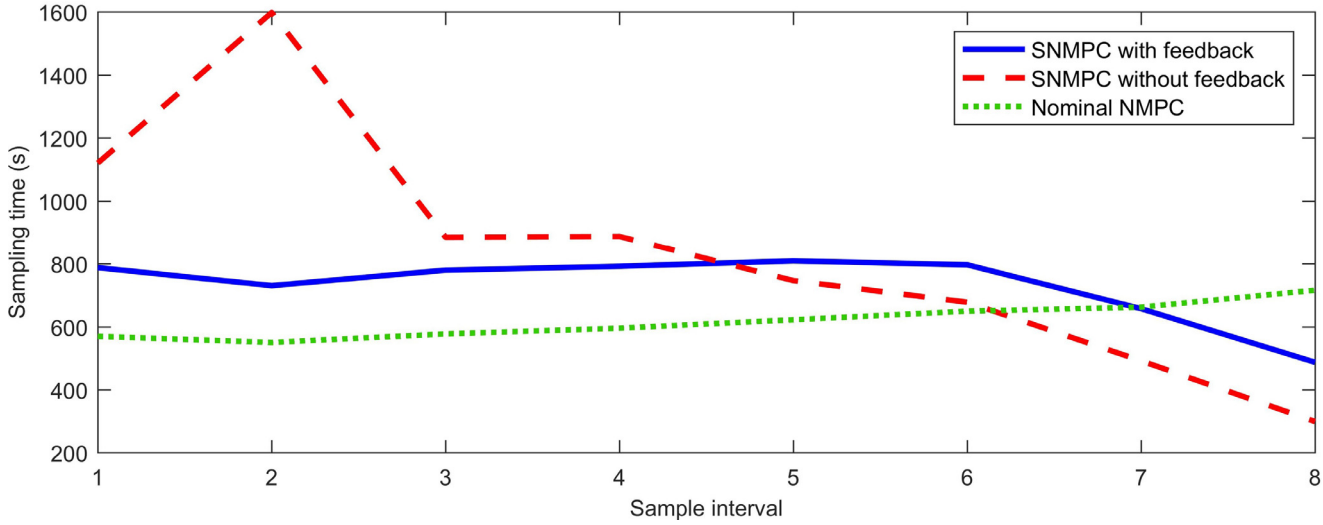

Fig. 9. Changes in sampling time for each sampling interval and algorithm variation.

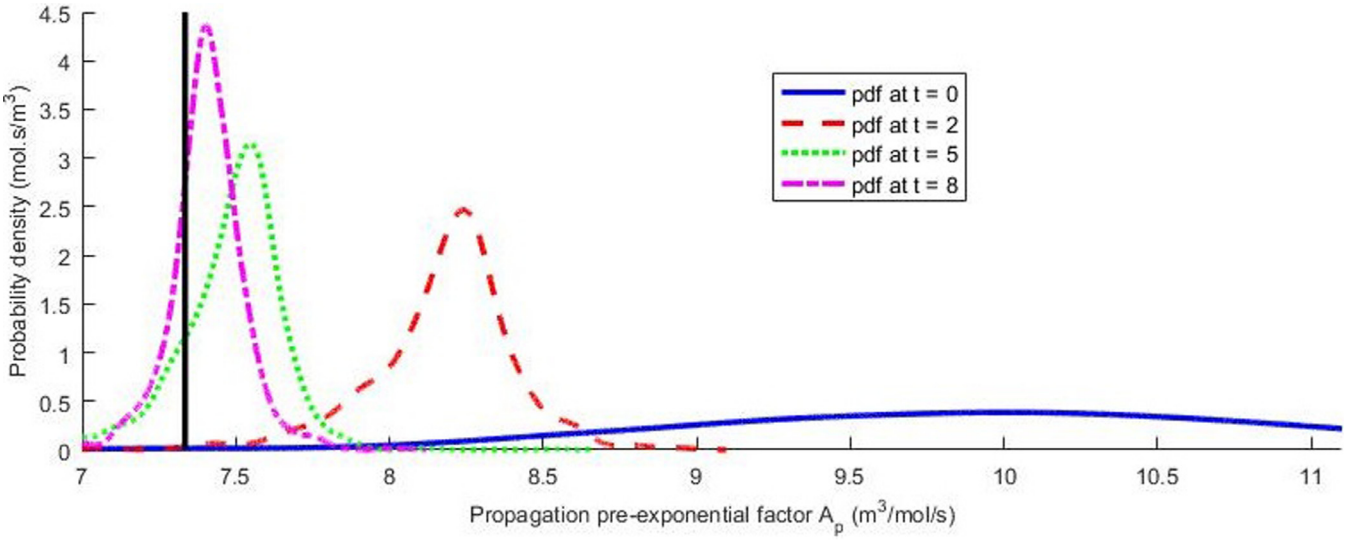

Fig. 10. Probability density function evolution for the propagation pre-exponential factor in the case of SNMPC with feedback.

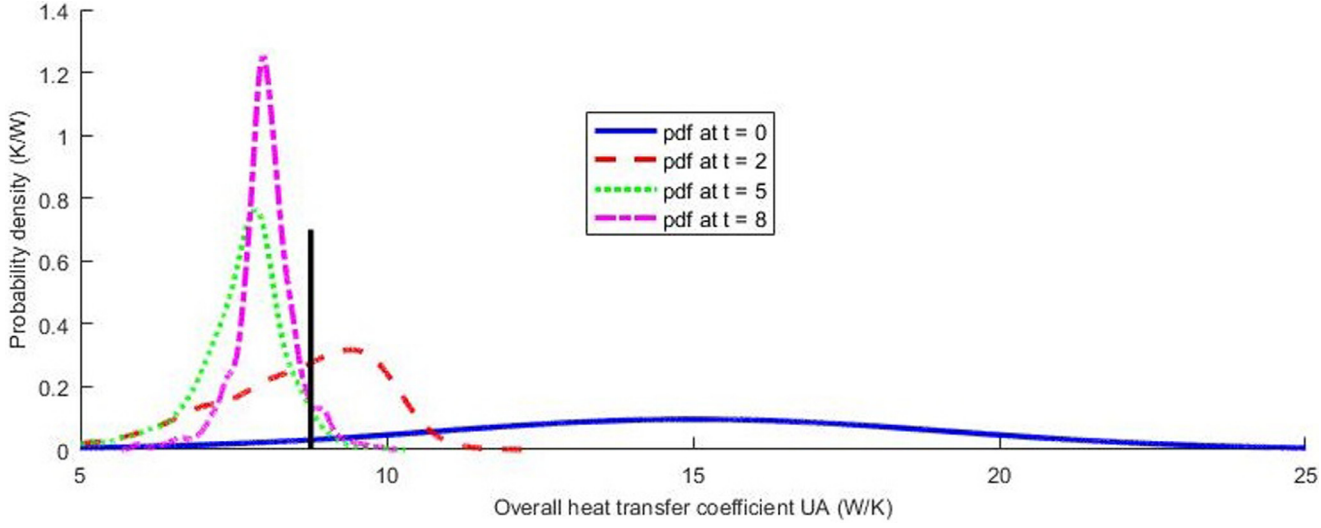

Fig. 11. Probability density function evolution for the overall heat transfer coefficient in the case of SNMPC with feedback.

in the reactor due to the open-loop growth of the uncertainty. This is further highlighted in Figs. 7 and 8, where the SNMPC without feedback keeps the Monomer feed rate and cooling water temperature at its lower bound for much longer than the other two algorithms. In addition it can be seen that the nominal NMPC overshoots the constraint slightly, while the SNMPC algorithms keep a reasonable distance to the constraint to prevent this.

- Fig. 4 shows the evolution of the monomer concentration. While the nominal NMPC and the SNMPC with feedback operate at a rather steady amount of monomer until it is reduced due to the second terminal constraint, the SNMPC without feedback increases it considerably due to its initial conservativeness. In addition it can be seen that both SNMPC algorithms have a longer "reduction" phase, which is due to considering the uncertainty in the problem. In fact the nominal NMPC algorithm contains 90ppm too much of the monomer in the final batch, while the SNMPC algorithms overshoot the constraint slightly.
- In Fig. 6 the evolution of the first polymer moment is shown, for which similar observations can be made as in Fig. 4. The nominal and SNMPC with feedback approach the constraint steadily, while the SNMPC without feedback takes longer due to its conservativeness and consequently low feedrate initially, see Fig. 7. Again while the nominal NMPC reaches the constraint exactly, both SNMPC algorithms overshoot the constraint to account for the uncertainty present. The final batch of the nominal NMPC has an NAMW that consequently is 0.1 kmol too small.
- It can be seen that the trajectories have different time lengths. The longest batch time is given by the SNMPC without feedback with a time of 6800 seconds due its relatively slow start resulting from the initially large open-loop uncertainties. By disregarding the uncertainties the nominal NMPC algorithm is able to have the shortest batch time with 5000 s, which however leads to it violating both terminal constraints. The SNMPC with feedback is intermediary with a batch time of 5900 s, since it considers the uncertainties present but does not have the problem of open-loop growing uncertainties.
- In Fig. 9 the variation of the sampling times is shown. The nominal NMPC has relatively consistent sampling times, since the reduction in uncertainty has no effect on its constraints. The two SNMPC algorithms on the other hand show an overall reduction of the sampling time, since the uncertainty is lowered from the PCE state estimator update. The SNMPC without feedback is as expected significantly more conservative initially and also shows a more dramatic response to the uncertainty reduction.
- In Figs. 10 and 11 the probability density functions of the uncertain parameters A_p and UA are shown for SNMPC with feedback at different discrete times. In both cases the initial distribution is very broad and quickly approaches the true value. Nonetheless even at $t = 8$ a certain amount of biasness remains in particular for UA. While this is accounted for in the SNMPC algorithms, it is ignored by the nominal NMPC algorithm, which only considers the mean of the distribution.

8.2. Monte Carlo simulations

Next we run 100 closed-loop MC simulations of the same case study applying the outlined algorithms by sampling the initial condition and the disturbances independently. The results of these MC simulations are summarised in Figs. 3–8. Figs. 3–5 show the probability density estimation of NAMW, the ppm of the monomer and the batch time respectively. Figs. 6–8 show the temperature trajectories of the 100 MC simulations for SNMPC with feedback, SNMPC without feedback and the nominal NMPC respectively. Based on these results the following observations can be made:

- Fig. 12 shows that for both SNMPC variations the constraint on the NAMW given by the vertical black line is not violated by any of the MC simulations despite the uncertainty present. The nominal NMPC algorithm on the other hand violates the constraint in 46% of the closed-loop simulations.
- Fig. 13 shows again that both SNMPC algorithms do not violate the constraint on the ppm of the monomer frequently or to a significant extent. The algorithm SNMPC with feedback violated this constraint in 3% of the simulations, while without feedback this constraint was violated in 2% of the simulations. In contrast the nominal NMPC contained too much monomer in the final batch in 53% of the simulations.
- Fig. 14 illustrates the trade-off for the more robust behaviour from the SNMPC algorithm compared to their deterministic counterpart. While the nominal NMPC requires an average batch time of 4900 s, the SNMPC with feedback needs approximately 7000 s on average. The SNMPC without feedback requires the largest batch times on average of 7400 s. In addition, this illustrates that the feedback leads to a reduction of batch times of about 5% with the same guarantees.
- Figs. 15–17 illustrate the improved temperature control of the SNMPC algorithms compared to the nominal NMPC. While the

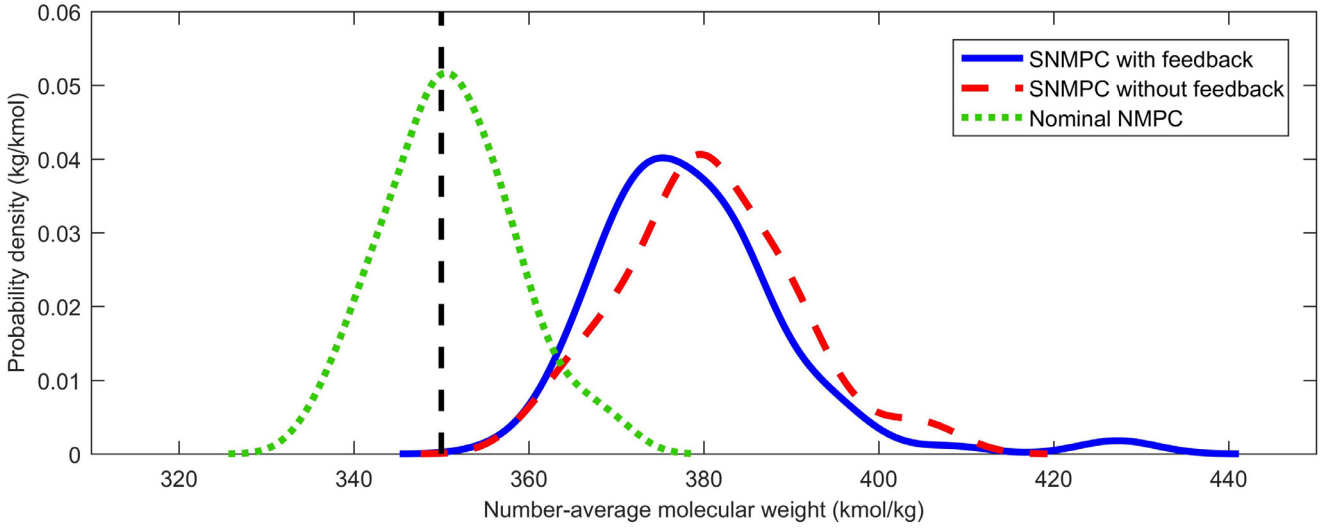

Fig. 12. Probability density of NAMW based on 100 MC simulations.

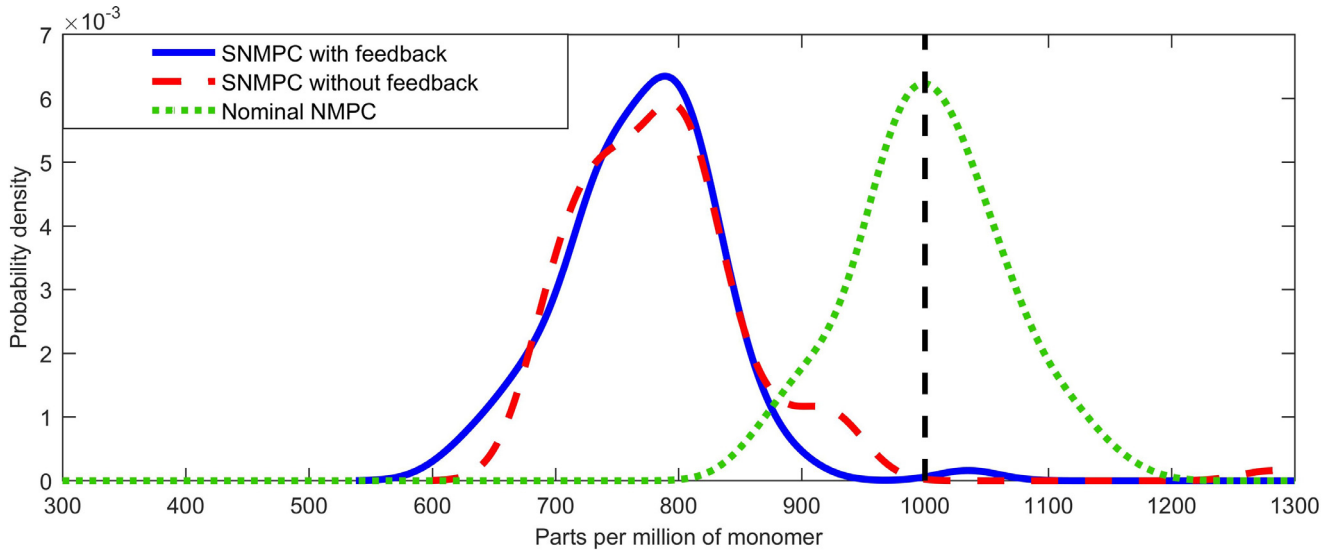

Fig. 13. Probability density of part per million of the monomer based on 100 MC simulations.

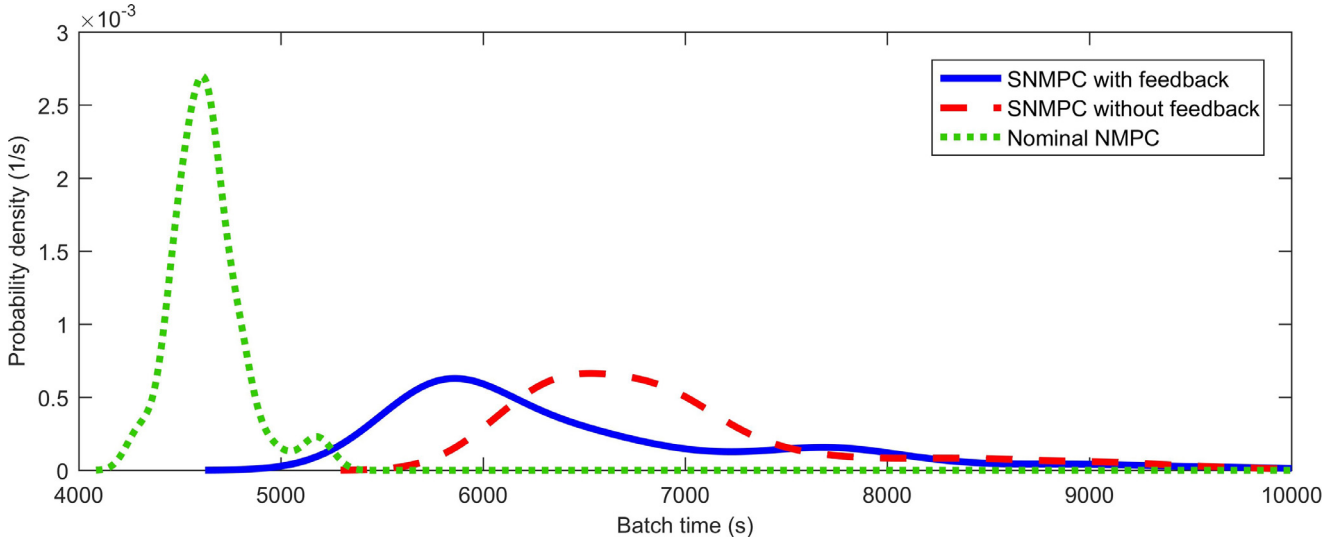

Fig. 14. Probability density of the batch times based on 100 MC simulations.

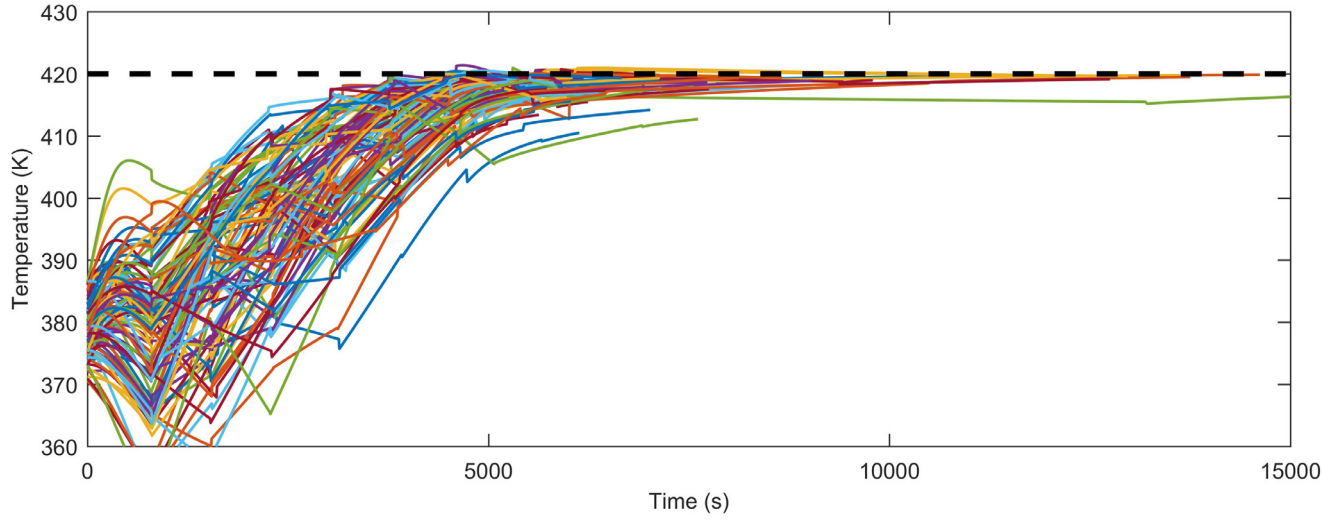

Fig. 15. Temperature trajectories of 100 MC simulation for SNMPC with feedback.

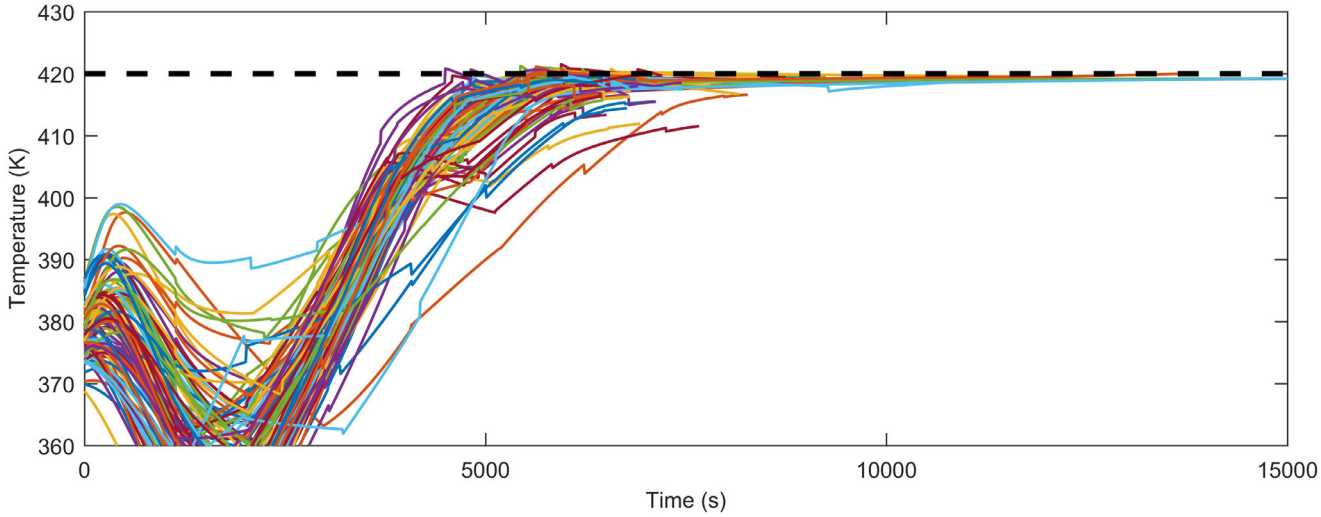

Fig. 16. Temperature trajectories of 100 MC simulation for SNMPC without feedback.

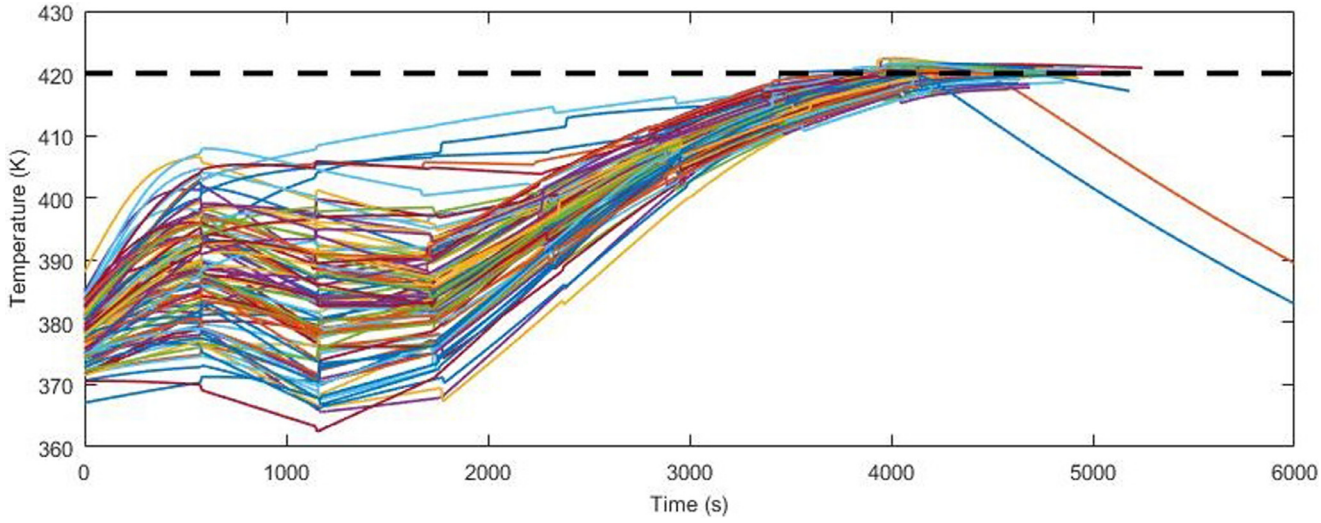

Fig. 17. Temperature trajectories of 100 MC simulation for nominal NMPC.

Table 2
The mean and standard deviation computational times for solving the sh-SNMPC OCP from 100 MC simulations.

sh-NMPC variation	Mean (s)	Standard deviation (s)
SNMPC with feedback	11.5	9.8
SNMPC without feedback	5.7	4.5
Nominal NMPC	0.27	0.1

nominal NMPC violates the temperature control 73% of the time, the SNMPC without feedback breaks it 30% and with feedback 14% of the time. Overall it can be said that the uncertainty has a small effect on the temperature constraint. The relatively large number of violations from the SNMPC variants can be possibly attributed to the inaccuracy of the linearization matrices in Eq. (80), although the extent of the constraint violation is considerably lower than the nominal NMPC.

- In Table 2 the computational times of the SNMPC algorithms and the nominal NMPC are shown. While SNMPC with feedback is significantly less conservative, it does require on average twice the computational time as the SNMPC without feedback. The nominal NMPC is as expected 20 times faster, since it is based on a much smaller optimization problem without scenarios and linearization propagation matrices.

9. Conclusions

In conclusion a new algorithm has been proposed for output feedback sh-SNMPC for batch processes. The algorithm is able to account for parametric uncertainties, state estimation errors and additive disturbance noise. PCEs are utilised to represent the probability distributions of the states and uncertain parameters, which are updated at each sampling time using a PCE nonlinear state estimator employing noisy output measurements. This PCE representation is then exploited in a SNMPC formulation, which accounts for this uncertainty using PCEs and considers the additive disturbance noise by employing linearization in conjunction with the law of total probability. To reduce the conservativeness the algorithm optimizes not only over open-loop control actions, but also over a time-invariant linear feedback gain. The objective and constraints were based on general nonlinear functions. The aim was set to minimise the objective in expectation, while adhering the constraints in probability to maintain feasibility. For verification purposes a semi-batch reactor case study was used, which showed that the SNMPC framework is able to control the system despite the uncertainties on the initial condition and additive disturbance noise. In particular, ignoring the uncertainty information leads to approximately 50% constraint violations of the terminal constraints

and to 70% violation of the temperature constraint. Further, considering feedback in the SNMPC formulation leads to on average 5% lower batch times with the same guarantees.

Acknowledgments

Eric Bradford gratefully appreciates BASF for hosting his placement over the course of the Marie-Curie project and the helpful input and discussions for this work. This project has received funding from the European Unions Horizon 2020 research and innovation programme under the Marie Sklodowska-Curie grant agreement No 675215.

References

Alamir, M., 2018. On the use of supervised clustering in stochastic NMPC design. arXiv:1811.09069

Andersson, J.A.E., Gillis, J., Horn, G., Rawlings, J.B., Diehl, M., 2018. Casadi: a software framework for nonlinear optimization and optimal control. Math. Program. Comput. 1–36.

Bavdekar, V.A., Mesbah, A., 2016. A polynomial chaos-based nonlinear Bayesian approach for estimating state and parameter probability distribution functions. In: American Control Conference (ACC), 2016. IEEE, pp. 2047–2052.

Bavdekar, V.A., Mesbah, A., 2016. Stochastic nonlinear model predictive control with joint chance constraints. IFAC-PapersOnLine 49 (18), 270–275.

Bemporad, A., Morari, M., 1999. Robust model predictive control: a survey. In: Robustness in Identification and Control. Springer, pp. 207–226.

Bertsekas, D. P., 2011. Dynamic programming and optimal control 3rd edition, volume II.

Biegler, L.T., 2010. Nonlinear programming: concepts, algorithms, and applications to chemical processes. Siam 10.

Bradford, E., Imsland, L., 2018. Economic stochastic model predictive control using the unscented kalman filter. IFAC-PapersOnLine 51 (18), 417–422.

Bradford, E., Imsland, L., 2018. Stochastic NMPC of batch processes using parameterized control policies. Comput. Aided Chem. Eng. 44, 625–630.

Bradford, E., Imsland, L., 2018. Stochastic nonlinear model predictive control using Gaussian processes. In: 2018 European Control Conference (ECC). IEEE, pp. 1027–1034.

Bradford, E., Reble, M., Bouaswaig, A., Imsland, L., 2019. Economic stochastic nonlinear model predictive control of a semi-batch polymerization reaction. In: Dynamics and Control of Process Systems, including Biosystems – 12th DYCOPS. IFAC, p. accepted.

Bradford, E., Reble, M., Imsland, L., 2019. Output feedback stochastic nonlinear model predictive control of a polymerization batch process. In: 2019 European Control Conference (ECC). IEEE, p. accepted.

Buehler, E.A., Paulson, J.A., Mesbah, A., 2016. Lyapunov-based stochastic nonlinear model predictive control: Shaping the state probability distribution functions. In: 2016 American Control Conference (ACC). IEEE, pp. 5389–5394.

Cao, Y., 2005. A formulation of nonlinear model predictive control using automatic differentiation. J. Process Control 15 (8), 851–858.

Chen, H., Scherer, C.W., Allgower, F., 1997. A game theoretic approach to nonlinear robust receding horizon control of constrained systems. In: Proceedings of the 1997 American Control Conference. IEEE, pp. 3073–3077.

Dutta, P., Bhattacharya, R., 2010. Nonlinear estimation with polynomial chaos and higher order moment updates. In: American Control Conference (ACC), 2010. IEEE, pp. 3142–3147.

Eldred, M., Burkardt, J., 2009. Comparison of non-intrusive polynomial chaos and stochastic collocation methods for uncertainty quantification. In: 47th AIAA Aerospace Sciences Meeting including the New Horizons Forum and Aerospace Exposition. Aerospace Sciences Meetings, p. 976.

Fagiano, L., Khammash, M., 2012. Nonlinear stochastic model predictive control via regularized polynomial chaos expansions. In: 51st IEEE Conference on Decision and Control (CDC). IEEE, pp. 142–147.

Goulart, P.J., Kerrigan, E.C., Maciejowski, J.M., 2006. Optimization over state feedback policies for robust control with constraints. Automatica 42 (4), 523–533.

Hindmarsh, A.C., Brown, P.N., Grant, K.E., Lee, S.L., Serban, R., Shumaker, D.E., Woodward, C.S., 2005. SUNDIALS: Suite of nonlinear and differential/algebraic equation solvers. ACM Trans. Math. Softw. 31 (3), 363–396.

Homer, T., Mhaskar, P., 2018. Output-Feedback Lyapunov-Based predictive control of stochastic nonlinear systems. IEEE Trans. Autom. Control 63 (2), 571–577.

Jang, H., Lee, J.H., Biegler, L.T., 2016. A robust NMPC scheme for semi-batch polymerization reactors. IFAC-PapersOnLine 49 (7), 37–42.

Jia, B., Xin, M., Cheng, Y., 2012. Sparse-grid quadrature nonlinear filtering. Automatica 48 (2), 327–341.

Jung, T.Y., Nie, Y., Lee, J.H., Biegler, L.T., 2015. Model-based on-line optimization framework for semi-batch polymerization reactors. IFAC-PapersOnLine 48 (8), 164–169.

Kimaev, G., RicardezSandoval, L.A., 2017. A comparison of efficient uncertainty quantification techniques for stochastic multiscale systems. AIChE J. 63 (8), 3361–3373.

Kristoffersen, T.T., Holden, C., 2017. Model predictive control and extended Kalman filter for a gas-liquid cylindrical cyclone. In: Control Technology and Applications (CCTA), 2017 IEEE Conference on. IEEE, pp. 1248–1255.

Lee, J.H., Ricker, N.L., 1994. Extended kalman filter based nonlinear model predictive control. Ind. Eng. Chem. Res. 33 (6), 1530–1541.

Lee, S.H., Chen, W., 2009. A comparative study of uncertainty propagation methods for black-box-type problems. Struct. Multidiscip. Optim. 37 (3), 239.

Lucia, S., Finkler, T., Engell, S., 2013. Multi-stage nonlinear model predictive control applied to a semi-batch polymerization reactor under uncertainty. J. Process Control 23 (9), 1306–1319.

Maciejowski, J.M., 2002. Predictive Control: With Constraints. Pearson education.

Maciejowski, J.M., Visintini, A.L., Lygeros, J., 2007. NMPC for complex stochastic systems using a Markov chain Monte Carlo approach. In: Assessment and Future Directions of Nonlinear Model Predictive Control. Springer, pp. 269–281.

Madankan, R., Singla, P., Singh, T., Scott, P.D., 2013. Polynomial-chaos-based Bayesian approach for state and parameter estimations. J. Guidance Control Dyn. 36 (4), 1058–1074.

Mayne, D.Q., Kerrigan, E.C., Van Wyk, E.J., Falugi, P., 2011. Tubebased robust nonlinear model predictive control. Int. J. Robust Nonlinear Control 21 (11), 1341–1353.

Mesbah, A., 2016. Stochastic model predictive control: an overview and perspectives for future research. IEEE Control Syst. 36 (6), 30–44.

Mesbah, A., Huesman, A.E.M., Kramer, H.J.M., Nagy, Z.K., Van den Hof, P.M.J., 2011. Realtime control of a semiindustrial fedbatch evaporative crystallizer using different direct optimization strategies. AIChE J. 57 (6), 1557–1569.

Mesbah, A., Streif, S., Findeisen, R., Braatz, R.D., 2014. Stochastic nonlinear model predictive control with probabilistic constraints. In: 2014 American Control Conference. IEEE, pp. 2413–2419.

Mühlpfordt, T., Paulson, J.A., Braatz, R.D., Findeisen, R., 2016. Output feedback model predictive control with probabilistic uncertainties for linear systems. In: American Control Conference (ACC), 2016. IEEE, pp. 2035–2040.

Nagy, Z.K., Braatz, R.D., 2003. Robust nonlinear model predictive control of batch processes. AIChE J. 49 (7), 1776–1786.

Nagy, Z.K., Braatz, R.D., 2004. Open-loop and closed-loop robust optimal control of batch processes using distributional and worst-case analysis. J.Process Control 14 (4), 411–422.

Nagy, Z.K., Mahn, B., Franke, R., Allgöwer, F., 2007. Real-time implementation of nonlinear model predictive control of batch processes in an industrial framework. In: Assessment and Future Directions of Nonlinear Model Predictive Control. Springer, pp. 465–472.

Nayhouse, M., Tran, A., Kwon, J.S.-I., Crose, M., Orkoulas, G., Christofides, P.D., 2015. Modeling and control of ibuprofen crystal growth and size distribution. Chem. Eng. Sci. 134, 414–422.

Nie, Y., Biegler, L.T., Villa, C.M., Wassick, J.M., 2013. Reactor modeling and recipe optimization of polyether polyol processes: polypropylene glycol. AIChE J. 59 (7), 2515–2529.

Nie, Y., Biegler, L.T., Villa, C.M., Wassick, J.M., 2013. Reactor modeling and recipe optimization of ring-opening polymerization: block copolymers. Ind. Eng. Chem. Res. 53 (18), 7434–7446.

O'Hagan, A., 2013. Polynomial chaos: a tutorial and critique from a statistician's perspective. SIAM/ASA J. Uncertain. Quantif. 20, 1–20.

Patrinos, P., Sopasakis, P., Sarimveis, H., Bemporad, A., 2014. Stochastic model predictive control for constrained discrete-time Markovian switching systems. Automatica 50 (10), 2504–2514.

Paulson, J.A., Mesbah, A., 2017. An efficient method for stochastic optimal control with joint chance constraints for nonlinear systems. Int. J. Robust Nonlinear Control 1–21.

Rasoulian, S., Ricardez-Sandoval, L.A., 2015. A robust nonlinear model predictive controller for a multiscale thin film deposition process. Chem. Eng. Sci. 136, 38–49.

Sehr, M.A., Bitmead, R.R., 2017. Particle model predictive control: tractable stochastic nonlinear output-feedback MPC. IFAC-PapersOnLine 50 (1), 15361–15366.

Stein, M., 1987. Large sample properties of simulations using latin hypercube sampling. Technometrics 29 (2), 143–151.

Streif, S., Karl, M., Mesbah, A., 2014. Stochastic nonlinear model predictive control with efficient sample approximation of chance constraints. arXiv:1410.4535.

Valappil, J., Georgakis, C., 2002. Nonlinear model predictive control of enduse properties in batch reactors. AIChE J. 48 (9), 2006–2021.

Wächter, A., Biegler, L.T., 2006. On the implementation of an interior-point filter line-search algorithm for large-scale nonlinear programming. Math.Program. 106 (1), 25–57.

Weissel, F., Huber, M.F., Hanebeck, U.D., 2009. Stochastic nonlinear model predictive control based on Gaussian mixture approximations. In: Informatics in Control, Automation and Robotics. Springer, pp. 239–252.

Xiu, D., Karniadakis, G.E., 2003. Modeling uncertainty in flow simulations via generalized polynomial chaos. J.Computat.Phys. 187 (1), 137–167.

Yan, J., Bitmead, R.R., 2005. Incorporating state estimation into model predictive control and its application to network traffic control. Automatica 41 (4), 595–604.